BBA - Biomembranes 1862 (2020) 183337

Contents lists available at ScienceDirect

BBA - Biomembranes

journal homepage: www.elsevier.com/locate/bbamem

The monomers, oligomers, and fibrils of amyloid-β inhibit the activity of mitoBK$_{Ca}$ channels by a membrane-mediated mechanism

Yevheniia Kravenska[a,b,*], Hanna Nieznanska[c], Krzysztof Nieznanski[d], Elena Lukyanetz[b], Adam Szewczyk[a], Piotr Koprowski[a]

[a] Laboratory of Intracellular Ion Channels, Nencki Institute of Experimental Biology PAS, Pasteura str. 3, Warsaw 02-093, Poland
[b] Department of Biophysics of Ion Channels, Bogomoletz Institute of Physiology NASU, Bogomoletz str. 4, Kyiv 01-024, Ukraine
[c] Laboratory of Electron Microscopy, Nencki Institute of Experimental Biology PAS, Pasteura str. 3, Warsaw 02-093, Poland
[d] Laboratory of Molecular Basis of Cell Motility, Nencki Institute of Experimental Biology PAS, Pasteura str. 3, Warsaw 02-093, Poland

ARTICLE INFO

Keywords:
mitoBK$_{Ca}$ channel
Mitochondria
Amyloid-β
Alzheimer's disease
Patch-clamp technique

ABSTRACT

A causative agent of Alzheimer's disease (AD) is a short amphipathic peptide called amyloid beta (Aβ). Aβ monomers undergo structural changes leading to their oligomerization or fibrillization. The monomers as well as all aggregated forms of Aβ, i.e., oligomers, and fibrils, can bind to biological membranes, thereby modulating membrane mechanical properties. It is also known that some isoforms of the large-conductance calcium-activated potassium (BK$_{Ca}$) channel, including the mitochondrial BK$_{Ca}$ (mitoBK$_{Ca}$) channel, respond to mechanical changes in the membrane. Here, using the patch-clamp technique, we investigated the impact of full-length Aβ (Aβ$_{1–42}$) and its fragment, Aβ$_{25–35}$, on the activity of mitoBK$_{Ca}$ channels. We found that all forms of Aβ inhibited the activity of the mitoBK$_{Ca}$ channel in a concentration-dependent manner. Since monomers, oligomers, and fibrils of Aβ exhibit different molecular characteristics and structures, we hypothesized that the inhibition was not due to direct peptide-protein interactions but rather to membrane-binding of the Aβ peptides. Our findings supported this hypothesis by showing that Aβ peptides block mitoBK$_{Ca}$ channels irrespective of the side of the membrane to which they are applied. In addition, we found that the enantiomeric peptide, D-Aβ$_{1–42}$, demonstrated similar inhibitory activity towards mitoBK$_{Ca}$ channels. As a result, we proposed a general model in which all Aβ forms i.e., monomers, oligomers, and amyloid fibrils, contribute to the progression of AD by exerting a modulatory effect on mechanosensitive membrane components.

1. Introduction

Alzheimer's disease (AD) is a complex and irreversible neurodegenerative disorder manifested by cognitive and memory deterioration [1–3].

Numerous genetic, biochemical, biophysical, and cell biological studies support the concept that aggregation-prone amyloid-β (Aβ) peptides play a key role in the development of AD pathology [1,2,4]. Aβ readily forms amyloid – a stable fibrillar aggregate [1,2,5] in a process, called amyloidogenesis, which is strongly influenced by the length of the Aβ molecule [6]. For example, the major agent in AD is Aβ$_{1–42}$ – one of the most frequently found in the various aggregates in the brain of patients [7]. At the same time, the shortest aggregation-susceptible part of the molecule consists of only 10 amino acid residues – Aβ$_{25–35}$ [8]. For decades, induction of cytotoxicity was attributed predominantly to amyloid fibrils of Aβ [9]; however, recently it was demonstrated that unstable, transient assemblies of Aβ, called soluble oligomers, are much more deleterious [10–13].

Aβ in different aggregate forms can affect intracellular organelles [14]. In particular, a role for Aβ-induced mitochondrial pathology in AD has been postulated [15–17]. Many mitochondrial targets have been proposed for the peptide [18], and mitochondrial dysfunction has become a hallmark of Aβ-induced neuronal toxicity [19–21]. This could be the result of the formation of nonselective ion channels by Aβ oligomers [22] or Aβ interference with some channels in the mitochondrial membranes.

One of the targets of Aβ interference is the large-conductance calcium-activated potassium (BK$_{Ca}$) channel found in the mitochondria (mitoBK$_{Ca}$) of various animal tissues, including the brain and heart [23,24] that is implicated in cytoprotection during cardiopathology and neuropathology [25], cell apoptosis and cancer [26,27]. Even though mitoBK$_{Ca}$ channels perform cytoprotective functions during

* Corresponding author at: Laboratory of Intracellular Ion Channels, Nencki Institute of Experimental Biology PAS, Pasteura str. 3, Warsaw 02-093, Poland.
E-mail address: y.kravenska@nencki.edu.pl (Y. Kravenska).

https://doi.org/10.1016/j.bbamem.2020.183337
Received 28 December 2019; Received in revised form 25 April 2020; Accepted 28 April 2020
Available online 04 May 2020

neuropathology, the contribution of mitoBK$_{Ca}$ channels, as well as BK$_{Ca}$ channels in general, to AD remains unknown. Very few studies have been performed on isolated mitochondria in this context [28]. Other experiments conducted to study the effect of Aβ on BK$_{Ca}$ channels were carried out with its plasmalemmal isoform in whole neuronal cells [29–32].

The U-87 MG glioma cell line, because of the high expression level of BK$_{Ca}$ channels both in the plasma membrane and in mitochondria [23,33], is a convenient cell model to study the physiological role of this channel. This study aimed to establish the effect of Aβ$_{1–42}$ on the mitoBK$_{Ca}$ channels in human U-87 MG astrocytoma cells and to determine its possible mechanisms. The mitoplast patch-clamp technique was used as the method of studying mitoBK$_{Ca}$ channel activity. We conducted comprehensive research, which led to the first description of the inhibitory effect of monomers, oligomers, and fibrils of the three types of Aβ (Aβ$_{1–42}$, Aβ$_{25–35,}$ D-enantiomeric Aβ$_{1–42}$). We found that all forms and types of Aβ inhibited the mitoBK$_{Ca}$ channel, and we concluded that the main mechanism of mitoBK$_{Ca}$ channel blocking was the interaction of Aβ with the mitochondrial membrane. These results improve our understanding of the molecular mechanisms underlying AD that can contribute to the development of potential methods for the prevention and treatment of this pathology.

2. Materials and methods

2.1. Media and cell culture

Human astrocytoma U-87 MG cells were cultured in Dulbecco's modified eagle medium (DMEM) with 4.5 g/l glucose (Laboratory of General Chemistry, Ludwik Hirszfeld Institute of Immunology and Experimental Therapy, Polish Academy of Sciences) supplemented with 10% fetal bovine serum (FBS; Gibco, USA), 100 μM/ml penicillin (Sigma-Aldrich), 100 μg/ml streptomycin (Sigma-Aldrich) and 2 mM L-glutamine (Gibco, USA) at 37 °C in a humidified atmosphere with 5% CO_2. The cells were usually reseeded every third day.

2.2. Preparation of Aβ monomers, oligomers, and fibrils

Aβ$_{1–42}$ (cat. # A-1163-2, rPeptide https://www.rpeptide.com/_code/_dyn_images/products/specs/A-1163–Beta-Amyloid-1-42.pdf-new.pdf), Aβ$_{25–35}$ (cat. # A-1060-1, rPeptide, Fig. S1) and Aβ$_{1–42}$ (cat. # AG968, Merck, Fig. S2) peptides were purchased from Analytik Jena AG and Merck, respectively. The D-enantiomer of Aβ$_{1–42}$ was synthesized by LifeTein (cat. # 0200046, Fig. S3). Dried samples were dissolved in hexafluoro-2-propanol (HFIP) and divided and placed into Eppendorf tubes. HFIP was evaporated overnight at room temperature. The dried peptide films were stored in Eppendorf tubes and maintained at −80 °C until use.

To prepare monomers, the peptide film was dissolved in 100 μl of 10 mM NaOH and sonicated (10 × 10 s at 25% output intensity; sonicator Q125, Qsonica) on ice [34]. Each sample was kept on ice and used in experiments the same day. To confirm the monomeric state of the peptide, the transmission electron microscopy (TEM) micrograph was taken immediately after dissolving of Aβ$_{1–42}$ (Fig. S4A).

For the preparation of oligomers, the monomers were diluted to 20 μM in the patch-clamp high calcium buffer (150 mM KCl, 10 mM 4-(2-hydroxyethyl)-1-piperazineethanesulfonic acid (HEPES), and 100 μM $CaCl_2$ at pH = 7.2) and incubated for 2 h at 37 °C in a Thermomixer C (Eppendorf) with 10-sec orbital shaking (400 rpm) every 20 min [34]. The sample was kept at room temperature and used in experiments within 1 h of preparation. The TEM micrograph of Aβ$_{1–42}$ oligomers incubated for an additional 1 h indicates that the oligomers were stable within this period (Fig. S4B).

To obtain amyloid fibrils, the incubation time was extended for at least 24 h for Aβ$_{1–42}$ and D-Aβ$_{1–42}$ and for at least 72 h for Aβ$_{25–35}$. Fibrils were centrifuged at 108000 *g*, 25 °C for 30 min (Sorvall MX 120 Micro-Ultracentrifuge, Thermo Fisher Scientific) followed by resuspending in fresh patch-clamp high calcium buffer. Protein concentration was determined by the bovine serum albumin (BSA) method.

To study effects of Aβ peptides on mitoBK$_{Ca}$ channel activity (patch-clamp experiments), the same final concentration range (0.1–5 μM) was used for all types of monomeric peptides and their aggregate derivatives. The concentration of oligomers and fibrils referred to the concentration of the (monomeric) peptide used for their production.

2.3. Measurements of thioflavin T fluorescence

To monitor Aβ aggregation kinetics, peptides (20 μM) were incubated at 37 °C in the high-calcium patch-clamp buffer (150 mM KCl, 10 mM HEPES, and 100 μM $CaCl_2$ at pH = 7.2) containing 10 μM thioflavin T (ThT) in 96-well plates (Bio-One, Greiner). Fluorescence was measured for 24 h in a plate reader (Infinite 200Pro, Tecan) at 37 °C with 10-s orbital shaking every 20 min [34]. The ThT fluorescence was measured at 485 nm at an excitation wavelength of 440 nm.

2.4. Transmission electron microscopy

For TEM imaging, 400-mesh copper grids covered with Formvar and carbon (Ted Pella) were used. Ten microliters of sample were spotted on grids for 40 s. The grids were stained for 20 s with 1% (w/v) uranyl acetate (SPI Supplies), dried at room temperature and examined using a JEM 1400 high-performance transmission electron microscope (JEOL Co.) equipped with an 11-megapixel Morada G2 7 TEM camera (EMSIS GmbH) [34].

2.5. Isolation of mitochondria

Mitochondria were prepared from the human astrocytoma U-87 MG cell line as previously described with slight modification [35]. Cells from one to three 75 cm^2 culture flasks were collected in phosphate-buffered saline (PBS) and centrifuged at 800 *g* for 10 min (Centrifuge 5804 R, Eppendorf). The cell pellet was resuspended and homogenized with 8 gentle strokes with a homogenizer (No. 19, Kontes Glass) in a preparation solution (250 mM sucrose, 5 mM HEPES, and 1 mM ethylene-bis(oxyethylenenitrilo)tetraacetic acid (EGTA) at pH = 7.2). The homogenate was centrifuged at 9200 *g* for 10 min. The pellet was again resuspended and centrifuged at 780 *g* for 10 min. The supernatant was centrifuged at 9200 *g* for 10 min. Finally, the pelleted mitochondria were resuspended in 15–50 μl of the preparation solution. The protocol was performed at 4 °C.

2.6. Patch-clamp experiments

Patch-clamp experiments on mitoplasts were performed as described previously, with some modifications [35]. Briefly, mitoplasts were prepared from a 1–3 μl sample of human U-87 MG cells. The mitochondria were placed in 40 μl of hypotonic solution (5 mM HEPES and 100 μM $CaCl_2$ at pH = 7.2) for 2 min to induce swelling and disrupt the outer membrane (Fig. 1A). Then, 10 μl of hypertonic solution (1.5 M sucrose, 30 mM HEPES, and 100 μM $CaCl_2$ at pH = 7.2) was added to the medium. A high calcium solution was used (150 mM KCl, 10 mM HEPES, and 100 μM $CaCl_2$ at pH = 7.2) to fill the patch-clamp pipette. Mitoplasts (0.5–1 μl) were added directly to the recording chamber. They were easily recognizable by their size, shape, transparency, and the presence of a “cap”. Mitoplasts' membrane patches were excised by tapping the microelectrode assembly. The low-calcium solution (1 μM $CaCl_2$) contained the following: 150 mM KCl, 10 mM HEPES, 10 mM N-(2-hydroxyethyl)ethylenediaminetriacetic acid (HEDTA) and 1.32 mM $CaCl_2$ at pH = 7.2. While being mixed, all modulators were added directly to the recording chamber. In some experiments, 5–10 μM of the specific mitoBK$_{Ca}$ channel blocker paxilline (cat. # P2928, Sigma-Aldrich) was used. The procedure of washing

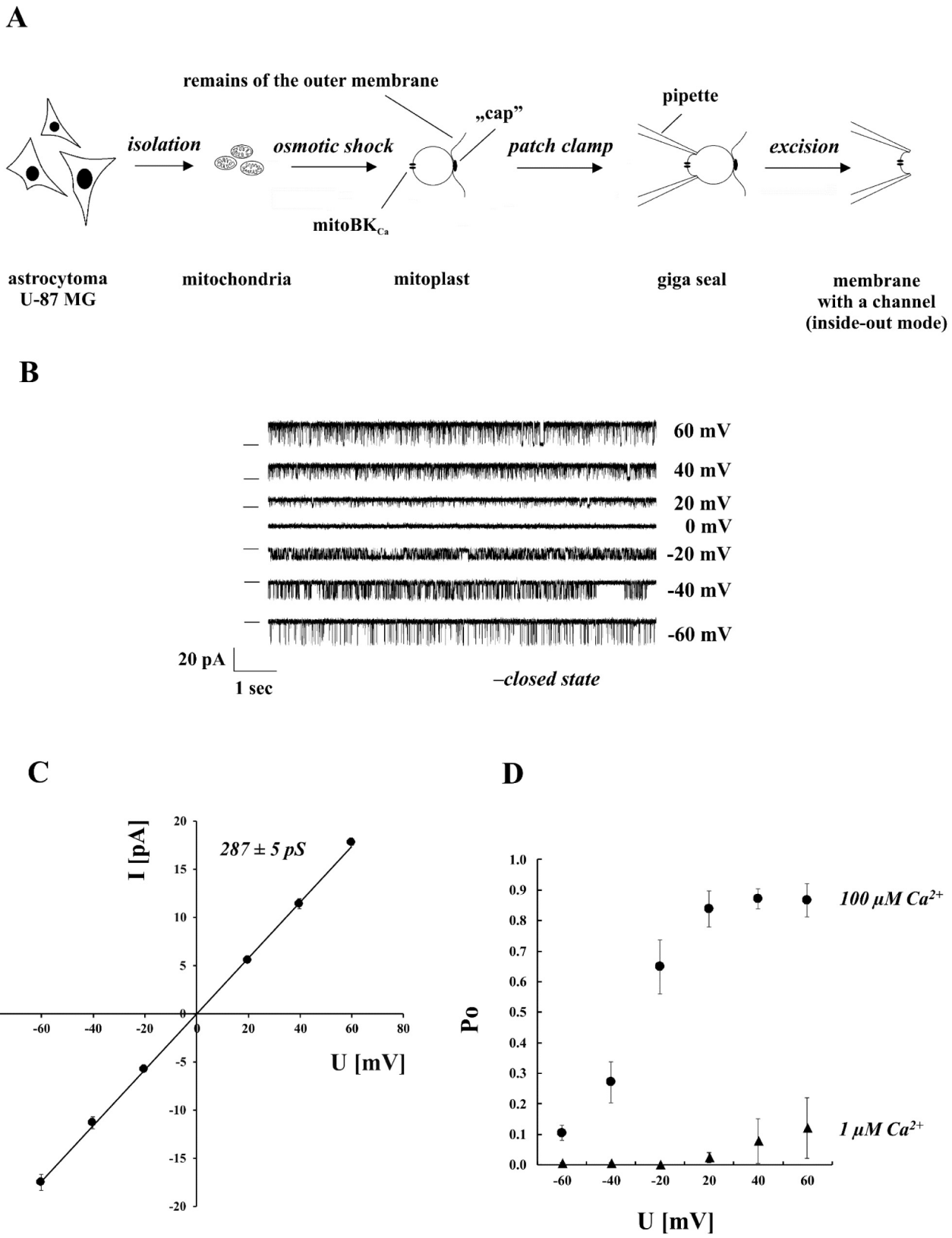

Fig. 1. Single-channel recordings of the activity of mitoBK$_{Ca}$ channel from astrocytoma U-87 MG cells. (A). Scheme of the preparation of U-87 MG cells mitochondria, mitoplasts and the patch-clamp experiment in the inside-out mode. (B). Typical activity of the mitoBK$_{Ca}$ channel at different voltages. "–" denotes the closed state of the channel (C). Current-voltage relationship of single-channel mitoBK$_{Ca}$ channel openings with a slope of 287 ± 5 pS (n = 4). (D). The open probability of single mitoBK$_{Ca}$ channels at different voltages in the presence of high (100 μM) and low (1 μM) concentration of calcium ions (n = 6). Data showed in (B–D) were obtained in the symmetric 150/150 mM KCl solution containing 100 μM Ca^{2+}(B, C) and 1 μM or 100 μM Ca^{2+} (D).

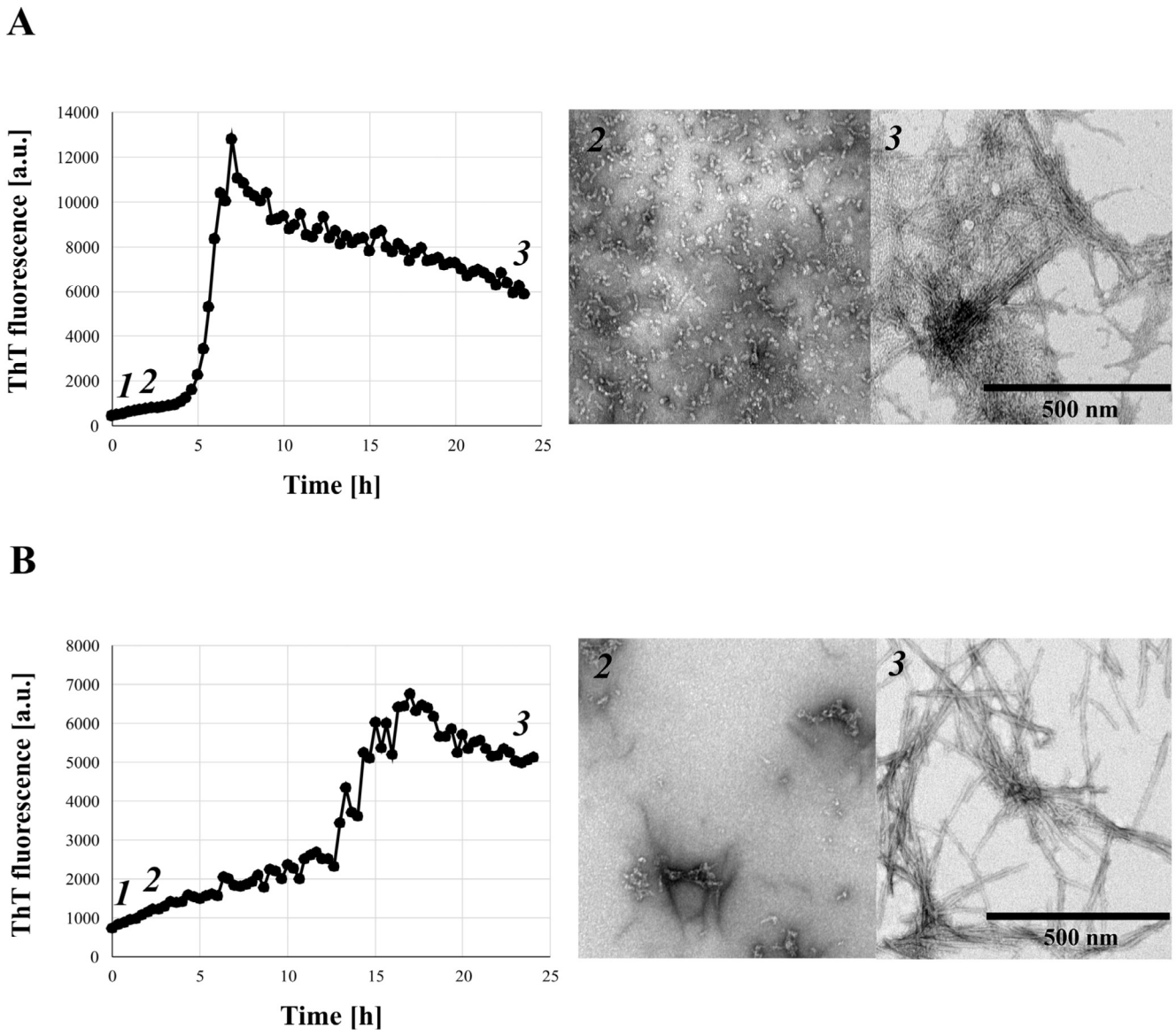

Fig. 2. Characterization of Aβ aggregates. Typical aggregation kinetics of $A\beta_{1-42}$ (A, left panel) and D-enantiomeric $A\beta_{1-42}$ (B, left panel). ThT fluorescence of 20 μM peptides was monitored during 24 h incubation at 37 °C. The monomers immediately after preparation (1), oligomers after 2 h (2) and fibrils after 24 h (3) of the incubation were used in patch-clamp experiments. Samples after 2 h (2) and 24 h (3) of the incubation were analyzed by electron microscopy (right panels).

out the mitoBK$_{Ca}$ channel from the applied substances was carried out by extensive flushing the bath chamber with not less than a 20-fold volume of the high calcium solution for 5–15 min. The experiments were performed in patch-clamp inside-out mode. Occasionally, however, channels were present in the opposite orientation, as described earlier [35]. The recordings of channel activity were obtained in the voltage range from −60 to +60 mV. The demonstrated voltages were opposite those applied to the patch-clamp pipette interior. Electrical connections were made using Ag/AgCl and an agar salt bridge (1.5 M KCl) electrodes. The current was recorded using a patch-clamp amplifier (Axopatch 200B, Molecular Devices Corporation). The pipettes, made of borosilicate glass, had a resistance of 10–15 MΩ and were pulled by either P-97 Flaming/Brown (Sutter Instruments) or PC-10 (Narishige) micropipette pullers. The conductance of the mitoBK$_{Ca}$ channel was calculated based on the current-voltage relationship. For the experiments, channels with a conductance of 250–300 pS were selected. The probability of channel opening (P_o, open probability) was calculated using the single-channel search mode of Clampfit 10.3 software. In the case of more than one channel in the patch, the NPo was first determined, and then the Po was calculated using the formula NPo/N, where N is the number of channels. Calculations were performed using short recordings (10 s) at −40 mV or segments of continuous recordings, lasting at least 90 s. The currents were subjected to low-pass filtering at 1 kHz and sampled at a frequency of 2.5 kHz. The recordings were filtered off-line by low-pass (at 250 Hz) and electrical interference filters. In figures showing single-channel recordings, "–" indicates the closed state of the channel.

2.7. Statistical analysis

For statistical analysis of the patch-clamp experiments, one-way analysis of variance (ANOVAs; with Tukey's post hoc test) or *t*-tests were used. To perform ANOVAs to create dose-response relationship curves and to determine half-inhibitory constant (IC_{50}) values, GraphPad Prism 4 software was used. Normalized Po was calculated as follows: $(Po_{A\beta}/Po_{control})*100\%$. The rate of Aβ inhibition was calculated as follows: $(Po_{control}–Po_{A\beta}/Po_{control})*100\%$. The data are represented as the mean ± standard deviation (SD) obtained from at

least three independent experiments. The P-value was considered to be significant for $P \leq 0.05$ (*, #) or $P \leq 0.01$ (**, ##).

3. Results

3.1. Monomers and fibrils of $A\beta_{25–35}$ inhibit the activity of mitoBK$_{Ca}$ channels

Previously published patch-clamp studies regarding the effects of Aβ peptides on BK$_{Ca}$ channels indicated their inhibitory action [31,32]. These experiments were carried out only with very short $A\beta_{31–35}$ and $A\beta_{25–35}$ peptides of undetermined aggregate form and applied directly to active plasma membrane BK$_{Ca}$ channels. The $A\beta_{25–35}$ peptide (GSNKGAIIGLM) with a short hydrophilic N- and a larger hydrophobic C-terminal part, and the ability of Aβ peptides including $A\beta_{25–35}$ to interact with membranes let us hypothesize that the effect on BK$_{Ca}$ channel was mediated by direct interaction with membrane. We used mitoBK$_{Ca}$ channels as a potential target and tool to check whether the inhibitory effect of Aβ peptides depends on their length and the aggregation status.

Patch-clamp experiments were carried out by a standard procedure (Fig. 1A) with mitochondria isolated from the human U-87 MG astrocytoma in which mitoBK$_{Ca}$ channel activity is frequently observed. This mitochondrial channel, characterized by high conductance and calcium ion dependence, was described previously [23]. The typical activity of mitoBK$_{Ca}$ channels at a range of voltages from −60 to +60 mV is shown in Fig. 1B–D. Short open times at negative voltages and long open times at positive voltages can be observed (Fig. 1B). The mean conductance of the mitoBK$_{Ca}$ channels was 287 ± 5 pS (Fig. 1C). One of the classic characteristics of the mitoBK$_{Ca}$ channel is its dependence on calcium ions [23]. Fig. 1D shows the full activity of the channel at Ca^{2+} concentration of 100 μM and its low activity when the Ca^{2+} concentration is decreased to 1 μM.

Aβ peptides are highly aggregation-prone, and thus, experiments were carried out with the peptides freshly dissolved in 10 mM NaOH and kept on ice. These peptides were either added directly to the recording chamber to investigate the impact of their monomeric forms or preincubated in the patch-clamp buffer for 2 h before the experiment to obtain oligomers and preincubated for > 24 h to obtain amyloid fibrils (Fig. S5).

Evidence from monitoring the aggregation state of $A\beta_{25–35}$ by ThT fluorescence revealed a slow monotonous increase without any lag phase (Fig. S5, left panel), which is not characteristic for amyloidogenesis of the full-length $A\beta_{1–42}$ (Fig. 2A). In the latter case, an approximate 4 h lag phase was observed, followed by a rapid increase in the fluorescence to the defined maximum. After approximately 7 h, a stable plateau was reached, which may indicate the completion of fibrillization (Fig. 2A, left panel). These differences in aggregation kinetics were reflected in different aggregate forms, as observed by TEM after 2 h and 24 h of incubation (Fig. S5, 2A, right panels). After 2 h of $A\beta_{25–35}$ incubation, no distinct structures could be observed despite the marked increase in ThT fluorescence, suggesting the presence of low molecular weight assemblies. On the other hand, after 24 h, $A\beta_{25–35}$ formed large ribbon- or sheet-like fibrils (Fig. S5, right panel), as also reported by others [36]. In contrast, the TEM images obtained for the $A\beta_{1–42}$ samples after 2 h and 24 h of aggregating revealed the presence of oligomers and fibrils (Fig. 2A, right panel). The preparations of oligomers consisted predominantly of short protofibrilar structures of 8–10 nm in diameter and length in the range of 10–40 nm. The preparations of fibrils contained typical amyloid aggregates of 25 nm in diameter, reaching up to 2 μm in length.

When we applied the $A\beta_{25–35}$ peptide in its monomeric form directly to active mitoBK$_{Ca}$ channels (Fig. S6), we observed an inhibitory effect at all voltages tested (Fig. S6A, right panel). However, the most apparent blocking was noticed at positive membrane voltages, at which, in control conditions, the channel had a high probability of opening (Po). The inhibitory effect of $A\beta_{25–35}$ monomers was concentration-dependent (Fig. S6C, D, E), and inspection of longer recordings (at least 90 s, −40 mV) in the presence of 1–5 μM $A\beta_{25–35}$ indicated that long-closed dwell times prevailed under these conditions, leading to occasional bursts of mitoBK$_{Ca}$ channel activity (Fig. S6C). Low concentrations of monomers (0.1–1 μM) had an inhibitory effect on the channels, but the minimum value to which the normalized Po was decreased equaled 53% (Fig. S6D). When 5 μM $A\beta_{25–35}$ was used, the Po dropped significantly, to a low of 36% (0.28 ± 0.16, $n = 4$, $P \leq 0.05$), in comparison to the control (0.75 ± 0.07, $n = 6$). This inhibitory effect was fully reversible by washing the $A\beta_{25–35}$ from the recording chamber. Under these conditions, the normalized Po was restored to 107% (0.80 ± 0.03, $n = 3$, $P \leq 0.05$) (Fig. S6C, D).

Similar effects were observed for $A\beta_{25–35}$ preincubated in the patch-clamp buffer for 2 h before experiments (data not shown); however, due to aggregate character and featureless appearance of $A\beta_{25–35}$ in the TEM images, we were not able to assign this Aβ preparation to any distinguishable aggregation form.

Surprisingly, the findings revealed that, in addition to the monomers, $A\beta_{25–35}$ fibrils inhibited the activity of mitoBK$_{Ca}$ channels at similar concentrations (Fig. S6D, Fig. S7), despite the different structures that these two forms represent. In particular, using the highest concentration of fibrils, we observed a decrease in normalized Po from 100% (0.75 ± 0.10, $n = 3$) to 36% (0.27 ± 0.12, $n = 3$), which was confirmed by statistical analysis ($n = 3$, $P \leq 0.05$) (Fig. S6D). This value reached a minimum of only 72% after the fibrils were applied at lower concentrations. Blocking mitoBK$_{Ca}$ channels by $A\beta_{25–35}$ fibrils was fully reversible, as washing out the experimental system restored channel activity to 101% (0.76 ± 0.145, $n = 3$, $P \leq 0.05$) (Fig. S7B, Fig. S6D).

Using dose-dependent relationship curves, we determined the half-inhibition constants (IC_{50}), which were equal to 0.6 μM and 1.45 μM for monomers and fibrils, respectively (Fig. S6E). Thus, we concluded that the $A\beta_{25–35}$ monomeric form is only slightly more active than the fibril form.

It has been established that $A\beta_{25–35}$ monomers bind to lipid bilayers, resulting in bilayer destabilization and channel formation [37]. Indeed, in our experiments, we were occasionally able to observe such membrane destabilization, which appeared as bursts of nonspecific activity that was different from the typical activity of mitoBK$_{Ca}$ channels (Fig. S6B). This phenomenon, however, was never observed for the $A\beta_{25–35}$ fibrils.

3.2. Monomers, oligomers, and fibrils of $A\beta_{1–42}$ inhibit the activity of mitoBK$_{Ca}$ channels

In the next step, we decided to extend our studies by including pathologically relevant full-length $A\beta_{1–42}$ in defined aggregate forms. As indicated above, the aggregation behavior of $A\beta_{1–42}$ (Fig. 2A) enabled us to analyze the impact of the monomers, oligomers, and amyloid fibrils on the mitoBK$_{Ca}$ channel activity.

As in the case of $A\beta_{25–35}$, the application of $A\beta_{1–42}$ monomers led to the strong inhibition of mitoBK$_{Ca}$ channels. Fig. 3A shows an example of such an experiment with the maximal $A\beta_{1–42}$ concentration used in the study (5 μM). The activity of the channel was recorded for 10 s at each membrane voltage indicated (−60 to +60 mV). The closure of the mitoBK$_{Ca}$ channel induced by $A\beta_{1–42}$ monomers also was dose-dependent (Fig. 3B–D). Continuous recordings (90 s or more) obtained at −40 mV made it possible to observe long-closed channel events over the entire range of the $A\beta_{1–42}$ concentrations (0.1–5 μM) (Fig. 3B). The blocking effect of the 5 μM $A\beta_{1–42}$ monomers was statistically significant (Fig. 3C): Po was equal to 0.33 ± 0.08 (normalized to 44%, $n = 5$), and for the control, it was 0.75 ± 0.07 ($n = 6$, $P \leq 0.01$). Such mitoBK$_{Ca}$ channel blocking was partially reversed after washing the peptide out of the chamber (Fig. 3B, C). In particular, the Po value returned to 0.50 ± 0.08 after the chamber was washed (67%,

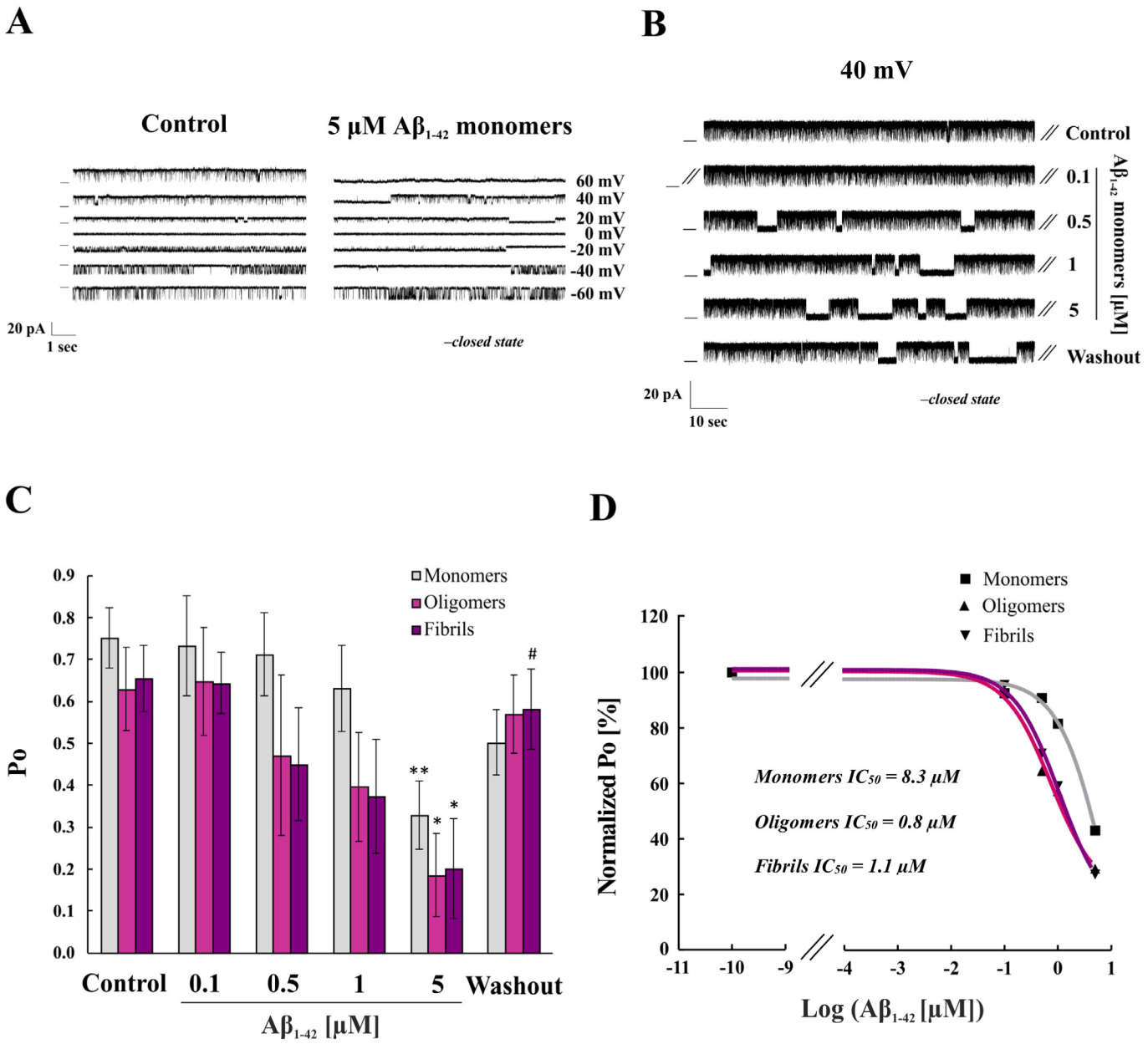

Fig. 3. Inhibition of the single-channel activity of the mitoBK$_{Ca}$ channels by Aβ_{1-42}. (A). Typical activity of mitoBK$_{Ca}$ channel at different voltages in the control conditions (left panel) or after the addition of 5 μM monomeric Aβ_{1-42} (right panel). (B). Typical recording of the single-channel activity of the mitoBK$_{Ca}$ channel after the addition of different concentrations of Aβ_{1-42} monomers. Channel activity was recorded continuously at −40 mV. (C). Dependence of mitoBK$_{Ca}$ channel open probability on the concentration of Aβ_{1-42} in the monomeric, oligomeric and fibrillar form (n = 3–7). Open probability was calculated for combined short and long recordings at −40 mV. (D). Dose-response relationship curves and IC$_{50}$ values of the mitoBK$_{Ca}$ channel inhibition by the monomers, oligomers, and fibrils of Aβ_{1-42}. Normalized Po was calculated as indicated in Experimental Procedures. Data shown in (A–D) were obtained in the symmetric 150/150 mM KCl solution containing 100 μM Ca^{2+}. In the control conditions, standard patch-clamp buffer without Aβ was used. "–" indicates the closed state of the channel. ** – P ≤ 0.01 (as compared to the control), # – P ≤ 0.05 (as compared to 5 μM Aβ_{1-42}).

normalized to the control, n = 5). When lower Aβ_{1-42} monomer concentrations were used (0.1–1 μM), the Po of the channel did not decrease to < 84% of the control (Fig. 3C). The IC$_{50}$ for the Aβ_{1-42} monomers, calculated with the normalized dose-response curve, was equal to 8.3 μM (Fig. 3D).

Examples of the short recordings at all voltages (Figs. S8A, S10A), as well as the long recordings taken at −40 mV (Fig. S9, upper panel, S10B), indicate that the effect of Aβ_{1-42} oligomers and fibrils was not only very similar but also more pronounced than that of the monomers. This finding was confirmed by the statistical analysis of the data (Fig. 3C). In particular, the decrease in Po caused by the maximal concentration of the oligomers and fibrils was greater than the caused when a similar concentration of monomers was used. For the oligomers, the normalized Po was 30% (0.19 ± 0.10, and for the control, it was 0.63 ± 0.10; n = 3–5, P ≤ 0.05). For fibrils, this value was equal to 31% (0.2 ± 0.12, n = 5), compared to the control (0.66 ± 0.08; n = 7, P ≤ 0.05). Lower concentrations of both aggregated forms were also effective, although to a lesser extent (a maximum Po of 63% for oligomers and 57% for fibrils) (Fig. 3C). An almost complete restoration of mitoBK$_{Ca}$ channel activity after Aβ_{1-42} was washed out of the chamber was observed in both cases (normalized to 91% for the oligomers, i.e., 0.57 ± 0.09, n = 5, and normalized to 89% for the fibrils, i.e., 0.58 ± 0.10, n = 7), although this difference was significant only for the fibrils (P ≤ 0.05) (Fig. 3C). The IC$_{50}$ for the oligomers and fibrils

(0.75 and 1.1 μM, respectively) was also noticeably lower than for the monomers, another confirmation of the higher effectiveness of these two forms (Fig. 3D).

Thus, we have proven that all aggregate forms of $A\beta_{1-42}$ cause closure of the $mitoBK_{Ca}$ channel. In this case, however, the monomers exhibited a less pronounced inhibitory effect.

In most patches, $mitoBK_{Ca}$ channels exhibit characteristic voltage dependence with short open-dwell times at negative membrane voltages and long open-dwell times at positive membrane voltages, as well as calcium ion sensitivity. However, in a small fraction of patches, the $mitoBK_{Ca}$ channels were not sensitive to calcium ions and demonstrated reversed voltage characteristics, evidence that, from time to time, we obtained patches in outside-out mode. Remarkably, the channels in the opposite orientation were also blocked by the oligomers and fibrils of $A\beta_{1-42}$ (Fig. S11). These observations confirmed our hypothesis that no specific peptide-protein interactions are involved, or $mitoBK_{Ca}$ channel blocking might be due to the binding of Aβ to mitochondrial membranes.

3.3. Enantiomeric forms of $A\beta_{1-42}$ exhibit the same inhibitory properties towards $mitoBK_{Ca}$ channels

To ultimately test our hypothesis that $mitoBK_{Ca}$ channels are inhibited as a consequence of Aβ-membrane interactions, we used enantiomeric $A\beta_{1-42}$ consisting of D-amino acids ($D\text{-}A\beta_{1-42}$) [38] In the ThT fluorescence assay, $D\text{-}A\beta_{1-42}$ aggregated with the characteristic lag phase (Fig. 2B, left panel), and the TEM images showed that the oligomers and fibrils of native form, $L\text{-}A\beta_{1-42}$, and $D\text{-}A\beta_{1-42}$, analyzed at the same time intervals (2 h and 24 h), were alike (right panels of Fig. 2).

In addition, the observed inhibitory effect of $D\text{-}A\beta_{1-42}$ against $mitoBK_{Ca}$ channels was similar to that of the $A\beta_{1-42}$. The $D\text{-}A\beta_{1-42}$ monomers, oligomers, and fibrils in identical concentrations blocked the channel both during the short-term (Figs. 4A, S8B, S12A) and long-term application (Figs. 4B, S9, lower panel, Fig. S12B). In particular, in the presence of 5 μM peptide in the recording chamber, the normalized Po decreased to the following values: 50% for monomers (0.40 ± 0.15 compared to the control of 0.81 ± 0.095, $n = 4$, $P \leq 0.01$), 28% for oligomers (0.22 ± 0.11 compared to the control of 0.77 ± 0.07, $n = 4, 6$, $P \leq 0.01$) and 23% for fibrils (0.165 ± 0.10 compared to the control of 0.71 ± 0.075, $n = 4, 6$, $P \leq 0.01$) (Fig. 4C). Other concentrations were also found to be effective, especially when the fibrils were used. In this case, the minimal normalized Po was equal to 46%. As with the previous two types of peptides, the inhibitory effect of $D\text{-}A\beta_{1-42}$ was almost completely reversible after washing it from the chamber (Figs. 4B, C, S9, lower panel, Fig. S12B). Thus, in the case of the monomers, the channel activity was restored to 97% (0.78 ± 0.07, $n = 4$, $P \leq 0.01$), after washing out the oligomers – to 114% (0.88 ± 0.06 $n = 3$, $P \leq 0.01$), and after washing out the fibrils – up to 96% (0.68 ± 0.07, $n = 5$, $P \leq 0.01$) (Fig. 4C). The calculated IC_{50} values were 2.7 μM, 1.5 μM, and 0.6 μM for the monomers, oligomers, and fibrils of $D\text{-}A\beta_{1-42}$, respectively (Fig. 4D).

Taken together, the data indicate that the monomeric form of $D\text{-}A\beta_{1-42}$ was slightly less effective than oligomers and fibrils of $D\text{-}A\beta_{1-42}$, but it still significantly blocked $mitoBK_{Ca}$ channels.

As a result of our studies, three forms of Aβ peptides in two or three aggregate states were compared. All the peptides had inhibitory activity against $mitoBK_{Ca}$ channels. Fig. 5 presents a comparison chart of the maximum channel inhibition by 5 μM Aβ peptides. $A\beta_{25-35}$ monomers and fibrils were equal in their inhibitory effects (64% and 63%, respectively). In the case of $A\beta_{1-42}$ and $D\text{-}A\beta_{1-42}$, the results showed similar tendencies. That is, the monomers were the weakest inhibitors (57% and 55%, respectively), while the oligomers (71% and 68%, respectively) and fibrils (73% and 79%, respectively) showed slightly more pronounced effects. Nevertheless, it should be emphasized that the overall range of inhibition (55%–79%) was not very wide. Additionally, no statistical significance for the rate of inhibition by the monomers vs. oligomers vs. fibrils was obtained. Taken together, these findings may be evidence of a common mechanism of blocking the $mitoBK_{Ca}$ channel by the studied peptides in all their forms, despite the physicochemical differences between their aggregate forms. We believe that the membrane-mediated inhibition of the studied channel explains the results described above.

4. Discussion

4.1. Alzheimer's disease and mitochondria

One of the most prominent hallmarks of AD is the impairment of mitochondrial function [39,40]. This impairment includes the upregulation of mitochondria-endoplasmic reticulum contacts in AD patients [41], disturbances to the lysosome-to-mitochondria signaling pathway [42], blocking of mitochondrial biogenesis and dynamics and, most notably, increased oxidative stress [43]. Consistent with these observations is the knowledge that Aβ is present not only in extracellular fluids but also accumulates in various intracellular compartments, including the endoplasmic reticulum, Golgi, endosomes, lysosomes [44], exocytotic vesicles and mitochondria [45,46], and it seems to profoundly impair the functions of some of these organelles, especially mitochondria [15,47,48] and lysosomes [49,50]. For example, the connection between Aβ-induced neuronal necrosis and the activity of the mitochondrial permeability transition pore has been demonstrated [20]. Furthermore, Aβ causes neuronal death by activating the caspase pathway, promoting mitochondrial fission, increasing reactive oxygen species production and disrupting mitochondrial membrane permeability [21].

4.2. The physiological role of mitochondrial BK_{Ca} channels as potential targets in AD

Ion channels are potential targets for Aβ in mitochondria taking into account the importance of their functions. BK_{Ca} channels are involved in many cellular processes [51]. Being in the plasma membrane, they regulate, for instance, the resting membrane potential, smooth muscle contraction, and neuron firing. In lysosomes, BK_{Ca} channel forms a complex with the transient receptor potential cation channel, member 1 (TRPML1) and provides positive feedback for Ca^{2+} release by TRPML1, enabling an influx of K^+ into the lysosomes and leading to hyperpolarization [52]. In mitochondria, the $mitoBK_{Ca}$ channel, which consists of pore-forming α subunits as well as modulatory β4 subunits, is additionally associated with complex IV of the respiratory chain and $mitoBK_{Ca}$ channel activity is modulated by electron transport chain substrates probably by a redox mechanism [33]. In this context interesting is a fact that activation of $mitoBK_{Ca}$ channels is an important factor for the recovery of cardiac function after ischemia/reperfusion injury when reactive oxygen species production is significantly increased [53,54]. It was found that gain-of-function mutations resulting in activation of $mitoBK_{Ca}$ channels reduced the amount of reactive oxygen species produced by complex I and complex II/III in transgenic mouse hearts after ischemia/reperfusion, and this production was further decreased with ischemic preconditioning. Although the presence of $mitoBK_{Ca}$ channels in brain mitochondria has been well-established [55,56], $mitoBK_{Ca}$ channel involvement in neuroprotection is inferred only from pharmacological studies [57,58].

In general, taking into account multiple functions played by BK_{Ca} channels localized in different compartments, as well as the presence of Aβ in these compartments, blocking the activity of BK_{Ca} channels by Aβ peptides must have important consequences. Nevertheless, only a few reports indicate the role of the BK_{Ca} channel located in the neuronal plasma membrane in the etiology of AD [31,59–61]. It was found that the application of $A\beta_{25-35}$ or $A\beta_{1-40}$ to acutely isolated rat neurons caused a reduction in whole-cell voltage-activated BK_{Ca} currents. This

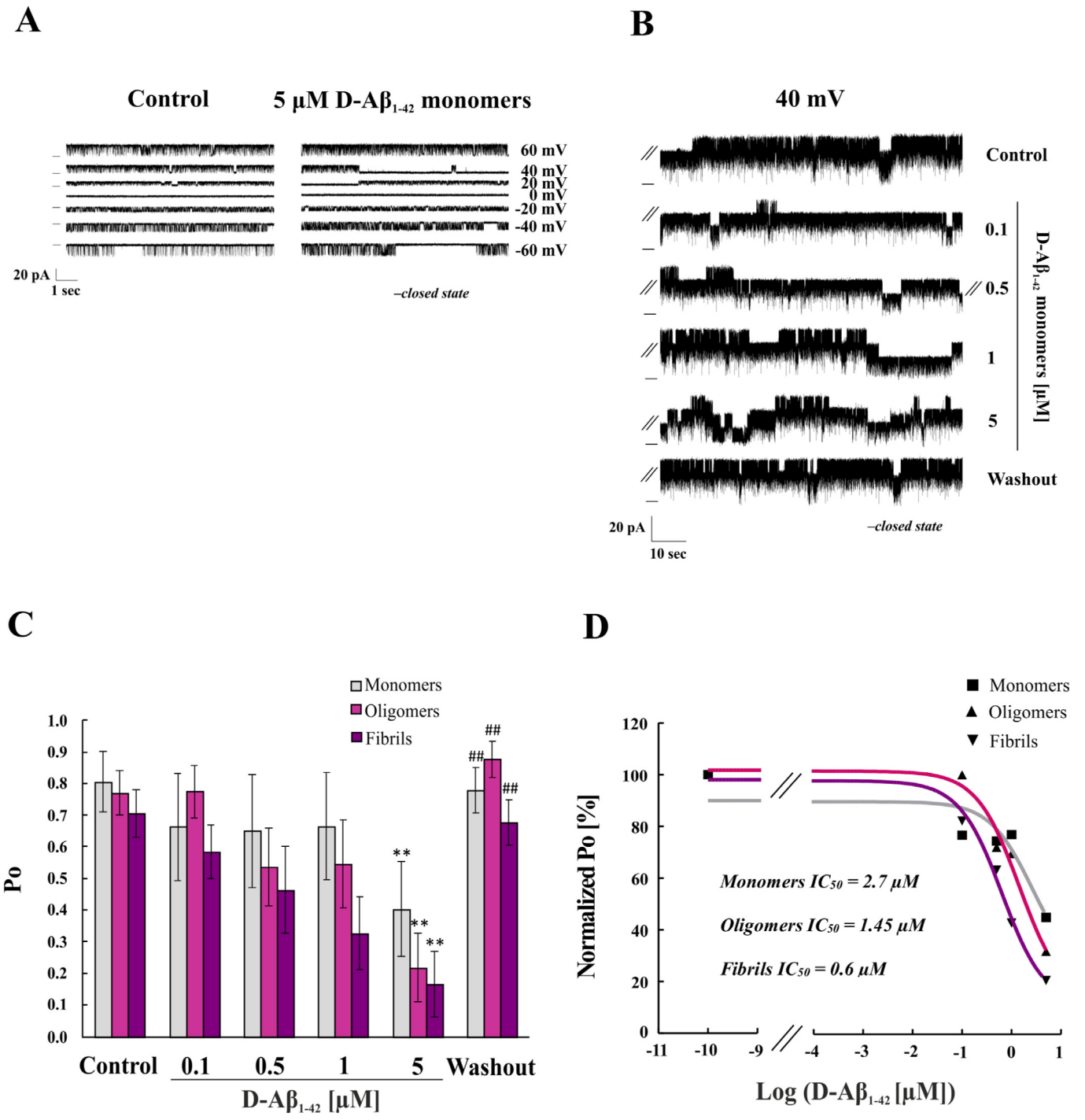

Fig. 4. Inhibition of the single-channel activity of mitoBK$_{Ca}$ channels by D-enantiomeric A$\beta_{1–42}$. (A). Typical activity of a mitoBK$_{Ca}$ channel at different voltages in the control conditions (left panel) and after addition of 5 μM monomeric D-A$\beta_{1–42}$ (right panel). (B). Typical recording of the single-channel activity of the mitoBK$_{Ca}$ channel after the addition of different concentrations of D-A$\beta_{1–42}$ monomers. (C). Dependence of mitoBK$_{Ca}$ channel open probability on the concentration of D-A$\beta_{1–42}$ in the monomeric, oligomeric and fibrillar form (n = 3–6). (D). Dose-response relationship curves and IC$_{50}$ values of mitoBK$_{Ca}$ channel inhibition by the monomers, oligomers, and fibrils of D-A$\beta_{1–42}$. Data shown in (A–D) were obtained in the symmetric 150/150 mM KCl solution containing 100 μM Ca^{2+}. ** – P ≤ 0.01 (as compared to the control), ## – P ≤ 0.01 (as compared to 5 μM of D-A$\beta_{1–42}$). See Fig. 3 for full description.

effect was specific to cholinergic but not to gamma aminobutyric acid-generating neurons [30]. Using the patch-clamp technique on inside-out excised membrane patches, Qi and Qiao [31] discovered that very short Aβ fragments (25–35) and (31–35) blocked the activity of the plasmalemmal BK$_{Ca}$ channels what was confirmed by recordings of the activity of BK$_{Ca}$ channels in whole hippocampal neurons [32]. Surprisingly, no full-length A$\beta_{1–42}$ was tested in these studies, nor was the mechanism or physiological significance investigated. Yamamoto et al. described A$\beta_{1–42}$-induced changes in Ca^{2+} influx into neurons via voltage-dependent Ca^{2+} channels and showed the dependence of this process on BK$_{Ca}$ modulators [59]. In addition, the role of calcium-activated potassium currents in hippocampus-dependent learning was investigated with hippocampal neurons of a TG2576 transgenic AD mouse model [62]. Other authors used the TgCRND8 mouse model of AD to show the connection between field excitatory postsynaptic potential and the activity of BK$_{Ca}$ channels in the hippocampus [63].

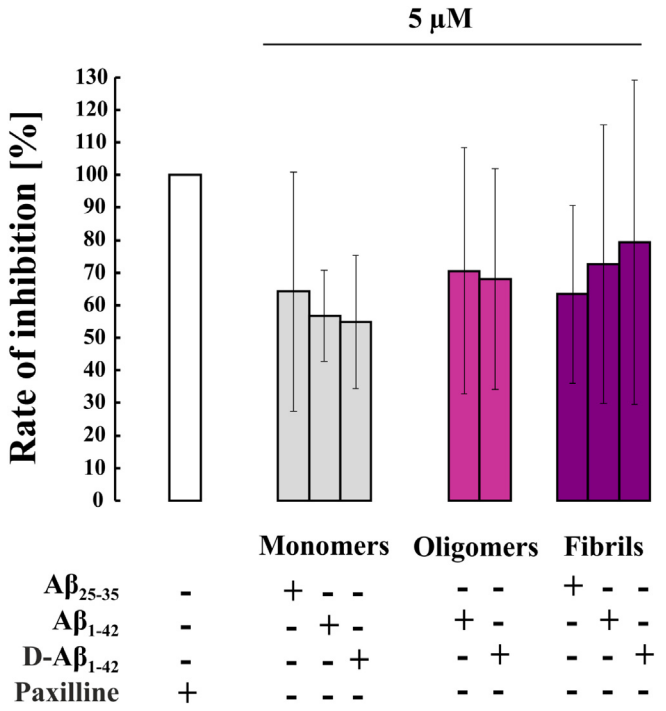

Fig. 5. Comparison of the inhibitory effect of all used in the study structural forms of $A\beta_{25-35}$, $A\beta_{1-42}$, and D-enantiomeric $A\beta_{1-42}$ in the concentration of 5 μM. The rate of inhibition of the single-channel activity of the $mitoBK_{Ca}$ channels was normalized to the control (standard patch-clamp buffer without Aβ addition) (n = 3–6) (see Materials and Methods). The effect of paxilline (5 μM) represents the full blocking of $mitoBK_{Ca}$ channel activity. Open probability was calculated for short and continuous recordings at −40 mV. Data were obtained in the symmetric 150/150 mM KCl solution containing 100 μM Ca^{2+}. P > 0.05 for the rate of inhibition by the monomers vs. oligomers vs. fibrils.

In the context of $mitoBK_{Ca}$ channels, Jafari and colleagues [28] described changes in the $mitoBK_{Ca}$ channel properties associated with β4 and α subunit expression and increased production of reactive oxygen species. The authors used an animal model of AD in which $A\beta_{1-42}$ was injected intracerebroventricularly.

4.3. Impact of membrane mechanics on the activity of BK_{Ca} channels

Several studies have shown that BK_{Ca} channels, both in the plasma membrane [64–68] and in the mitochondrial membrane [35], are mechanosensitive, meaning that their activity is dependent on the local tension within the membrane [69,70]. Most mechanosensitive channels open in response to mechanical stretching and bending of the membrane when some physicochemical parameters of the membrane are altered, including lipid packing and mobility or membrane thickness [71]. Indeed, it was shown that the activity of the BK_{Ca} channel is modulated by changes in bilayer thickness [72]. However, the same effects could be the result of the binding of cations such as Mg^{2+}, Ca^{2+}, and Gd^{3+} [73,74] and the insertion of small molecules into the membrane [75]. Gd^{3+} blocks the activity of BK_{Ca} channels [68], emphasizing the fact that this channel is influenced by the physical state of the membrane [76]. BK_{Ca} channels are activated by conical and amphipathic small molecules such as chlorpromazine [77], or ethyl-L-(((4-chlorophenyl)amino)oxo)-2-hydroxy-6-trifluoromethyl-1H-indole-3-carboxylate (CGS7184) [35,78]. They also open bacterial [79,80] and eukaryotic [81] mechanosensitive channels, underscoring their indirect (membrane-mediated) but not the direct (protein-mediated) mechanism. These data indicate that BK_{Ca} channels are sensitive to "unspecific" membrane modifiers.

4.4. Binding of Aβ to lipid membranes

Aβ may be considered as membrane modifying molecule. Numerous studies provide evidence that monomeric Aβ binds to lipid membranes. For instance, the results from small-angle neutron scattering and neutron membrane diffraction revealed that the monomeric Aβ could anchor to the negatively charged bilayers, affecting the lateral motion of the membrane lipids [82]. It also seems likely that Ca^{2+} ions can increase Aβ-bilayer interactions by making the dimyristoyl phosphatidylglycerol bilayer partially cationic and thus attractive to the anionic Aβ peptide [83]. Nuclear magnetic resonance spectroscopy performed at low temperatures to stabilize monomeric Aβ showed that initial interactions between Aβ and the lipid membranes are predominantly controlled by the surface features of the membrane rather than the hydrophobic characteristics [84]. It has been demonstrated that monomers of Aβ bind to membranes. Is it, however, true for all aggregate forms of Aβ, including amyloid fibrils? Indeed, not only the Aβ monomers [85], but also oligomers [86], and fibrils [87] bind to membranes, although the mechanisms of binding could differ between these forms. For instance, atomic force microscopy studies indicated that the Aβ fibrils embed laterally into the membrane, displacing the upper leaflet of the bilayer [86] and suggesting that the tension profile of the bilayer is affected. On the other hand, the Aβ oligomers impact the bilayer in a detergent-like fashion [86].

A number of studies point to membrane gangliosides (more specifically GM1) as significant players in binding and inducing the aggregation pathway of Aβ [88,89]. However, gangliosides are not normally detectable in mitochondrial membranes [90]. The studies by Sahoo et al. [91] with the use of lipid nanodiscs of different compositions showed that all of them promoted Aβ aggregation indicating that GM1 is not exclusively needed for this process. However, the presence of GM1 might be important for the outcome of Aβ interactions with the membranes. Sciacca et al. [92] demonstrated that membrane disruption by Aβ occurs by a two-step process – first, soluble oligomers bind to membranes to form small channel-like pores; second, Aβ fibril elongation results in membrane fragmentation through a detergent-like mechanism. Furthermore, it was shown that pore formation occurs at a lower level in the absence of gangliosides while membrane disruption by fibrils is completely dependent on gangliosides. It seems that binding of Aβ to mitochondrial membranes might have a different outcome in comparison to the process observed for the plasma membrane. In this case, mitochondrial membranes will induce aggregation of Aβ without the formation of channels or membrane disruption. Indeed, we did not observe in our electrophysiological study any membrane disruption with the native full-length $A\beta_{1-42}$.

Another key player in modulating the pathway of amyloid formation on the lipid bilayers seems to be its thickness [93] and aggregation of amyloids on bilayers can reduce local bilayer thickness via mechanical strain [94]. Binding of Aβ can also increase membrane viscosity and curvature. For instance, a study in which so-called viscosity-sensing fluorophores were employed revealed a decrease in bilayer viscosity upon incubation of giant unilamellar vesicles with $A\beta_{1-42}$ oligomers, while $A\beta_{1-42}$ fibrils did not affect their microviscosity [95]. It was proposed that fluorescent probe diffusion does not measure viscosity but the free volume of the membrane, which is related to the membrane tension [96] – indicating that Aβ alters this characteristic. In another study it was shown on cell-sized liposomes that Aβ monomers induced budding transformation of membrane domains indicating for changes in tension and curvature [97].

4.5. Mechanism of inhibition of $mitoBK_{Ca}$ by Aβ

In our studies, we observed inhibition of $mitoBK_{Ca}$ channel activity by all Aβ forms. We started experiments with the simplest amyloid beta fragment, $A\beta_{25-35}$, which previously was shown to inhibit plasmalemmal BK_{Ca} channels [31,32]. This short fragment was reported to be

present in AD patients' brains [98,99]. It is also an established model preserving the main features of Aβ – aggregation, and toxicity [100]. Both, short peptide $A\beta_{25–35}$ monomers and fibrils decreased the activity of $mitoBK_{Ca}$ channels. The $A\beta_{25–35}$ monomers were the most effective species in channel blocking, with an IC_{50} of 0.6 μM, i.e., they were > 10-fold more effective than $A\beta_{1–42}$ monomers. This fact was correlated with the membrane-destabilization potential of $A\beta_{25–35}$ monomers which formed active channels at concentrations ≤5 μM. Similar effect has not been observed for $A\beta_{1–42}$ in our experiments. $A\beta_{25–35}$ seemed to undergo oligomerization that differed from that of $A\beta_{1–42}$ since no visible lag phase was observed during the aggregation process. For this reason, no experiments with forms defined as $A\beta_{25–35}$ oligomers were reported in our study.

Likewise, above-mentioned $A\beta_{25–35}$, $A\beta_{1–42}$ inhibited $mitoBK_{Ca}$ channels. We noticed only small quantitative differences in the effectiveness of $mitoBK_{Ca}$ channel blocking, and these differences could depend on the Aβ aggregation state. The inhibition of the channels by $A\beta_{1–42}$ oligomers and fibrils was stronger when compared to the inhibition by the respective monomers. In particular, the affinity (characterized by IC_{50}), as well as the effect on $mitoBK_{Ca}$ channels at the maximal concentration (5 μM), for $A\beta_{1–42}$ monomers was approximately 1.5- to 10-fold lower than it was for the oligomers and fibrils. This observation is consistent with that of a study proving that the oligomeric Aβ adsorbs to liposomes or cortical homogenates to a greater extent than its monomeric form [101]. Thus, it seems that the conformation and aggregation states of Aβ are important in regulating the degree of interaction with lipid membranes. Solvent-exposed hydrophobic domains were detected in the oligomeric Aβ but were not present in either the monomeric Aβ or in mature amyloid fibrils [102].

It has to be noticed that the concentration of fibrils used in our experiments is based on the molar concentration of Aβ monomers. However, due to the polymeric structure of the fibrils, their effective molar concentration is several orders of magnitude lower. As a consequence, if a defined binding site on a $mitoBK_{Ca}$ channel protein was the target for both monomers and fibril binding, the fibrils would be several orders of magnitude less effective at inhibition than monomers. However, since both forms are effective to a similar extent, one can assume that the area or volume occupied by Aβ peptides determines their effectiveness, not their concentration level, further supporting the membrane-mediated mechanism explanation. It is also to be noticed that the $A\beta_{25–35}$ fibrils displayed notably different morphology in comparison to that of the fibrils of the full-length $A\beta_{1–42}$, nevertheless, both forms were effective towards $mitoBK_{Ca}$ channels to a very similar extent (IC_{50} of $A\beta_{25–35}$ and $A\beta_{1–42}$ fibrils equal to 1.45 and 1.1 μM, respectively).

In summary, it should be stressed that, despite the uncertainties of the mechanism by which Aβ alters properties of membranes [103] and the different modes of binding by different aggregate forms of Aβ, the mechanical properties of the membrane were profoundly affected by all of them. In addition, since each of these forms exhibits distinct structural features [104], it is not conceivable that Aβ binds to the $mitoBK_{Ca}$ channel directly at a defined site, instead, the membrane-mediated mechanism should be considered.

The definitive evidence for a membrane-mediated mechanism of Aβ peptide blocking of the $mitoBK_{Ca}$ channels is found in our experiments with the enantiomeric form of $A\beta_{1–42}$ (i.e., D-$A\beta_{1–42}$). Studies of this kind in different experimental systems have been previously carried out. For instance, it was found that D-$A\beta_{1–42}$ forms channels, with behavior in the lipid bilayer that was indistinguishable from that, described earlier for the L-Aβ enantiomer [102]. D-Aβ channels were blocked by Zn^{2+}, a known blocker of L-Aβ channels. Molecular dynamics simulations further verified the existence of β barrel-like Aβ channels with D- as well as L-enantiomers. Since these channels can directly mediate Aβ effects, even in the absence of direct receptor-peptide interaction, it was suggested that Aβ toxicity is mediated through a receptor-independent, nonstereoselective mechanism [105]. However, several in vitro studies with L- and D-Aβ enantiomers gave somewhat contradictory results. In a study by Cribbs et al. [38], both enantiomers induced similar toxicity in cultured hippocampal neurons. In contrast, in another study on cortical neurons, only L-$A\beta_{1–42}$ was neurotoxic, as indicated by the inhibition of long-term potentiation and phosphatidylserine was identified as a potential stereospecific target [106]. Similarly, in a study carried on PC12 cells, L-$A\beta_{1–42}$ induced approximately 40% of the maximum lactic acid dehydrogenase (LDH) release, whereas D-$A\beta_{1–42}$ was much less effective, inducing 10% of LDH release, indicating some stereospecific action [107]. Interestingly, the complete lack of stereospecificity was observed in the case of inhibition of the PIEZO1 channel by $A\beta_{1–42}$. The mechanosensitive PIEZO1 channel is gated by membrane tension and curvature [108,109]. Using fluid shear stress as a stimulus, Maneshi et al. [110] discovered that $A\beta_{1–42}$ monomers inhibit PIEZO1 channels at low femtomolar concentrations, while the $A\beta_{1–42}$ oligomers proved to be much less effective. Presumably, the impact of Aβ on PIEZO1 gating did not involve peptide-protein interactions since the D- and L-enantiomers had similar effects. Studies with fluorescently labeled Aβ and PIEZO1 revealed that Aβ can localize in the same regions of the membrane as PIEZO1 does, suggesting the modulation of cell membrane mechanics [111]. PIEZO1 is also inhibited by another membrane-binding peptide, GsMTx4, in a nonstereospecific way [112]. Both enantiomeric forms – the native L-GsMTx4 and the D-GsMTx4 – modify the gating of the PIEZO channels, which is a finding inconsistent with the lock-and-key model of ligand-protein interactions.

In the case of Aβ inhibition of $mitoBK_{Ca}$ channels by direct protein-peptide binding, one might expect that this interaction would be stereospecific. However, it was not observed in our experiments given that both enantiomers (L- and D-$A\beta_{1–42}$) were effective. Channel blocking was obtained for the monomeric, oligomeric and fibrillar forms of D-$A\beta_{1–42}$ with characteristics similar to the blocking attributed to $A\beta_{1–42}$. In contrast to our results there are studies on cholesterol derivative 24S-hydroxycholesterol, a membrane component, that blocks BK_{Ca} channels by stereospecific binding to channel protein within the membrane [113–115]. Taken together, these findings indicate the membrane-binding propensity of Aβ, but not specific Aβ structure, played a crucial role in $mitoBK_{Ca}$ channel blocking.

The importance of the action of Aβ on a membrane channel-forming protein as a target in mitochondria is underscored by the fact that we never observed ion channel activity of $A\beta_{1–42}$ itself, although the activity of such channels in the plasma membrane exposed to the oligomers of $A\beta_{1–42}$ has been reported and was attributed to $A\beta_{1–42}$ toxicity [22,86]. Our observation could be partially explained by the lack of GM1 ganglioside mentioned above or findings of a study by Wong et al. [116], who showed that membrane binding and pore formation by $A\beta_{1–40}$ proceeds in two distinct steps. In their investigation, oligomers of $A\beta_{1–40}$ interacted preferentially with negatively charged membranes in the gel, liquid-crystalline, and liquid-ordered phases, which changed the peptide conformation to a similar extent. However, membrane permeabilization was highly dependent on the fluidity/phase of the membrane, as a decrease in its fluidity was associated with reduced permeability. Therefore, under our experimental conditions at room temperature (c.a. 21 °C), $A\beta_{1–42}$ might not have been able to perforate the membrane patches. In agreement with this finding, $A\beta_{1–42}$ did not exhibit any effect on $\Delta\psi mt$ when incubated with isolated mitochondria at 30 °C, even at high concentrations [117]. This finding differs from that of $A\beta_{25–35}$, which frequently caused the destabilization of membrane patches and erratic currents in agreement with previous studies showing fast membrane permeabilization by this peptide [37]. In the end, we cannot exclude the possibility that ion channels are formed by oligomers of $A\beta_{1–42}$ in mitochondrial membranes in vivo at 37 °C; however, a growing number of new studies (showing that not only oligomers but also monomers and fibrils of $A\beta_{1–42}$ are toxic) have indicated that Aβ oligomer ion channel-related toxicity is not the only possible pathological mechanism in AD.

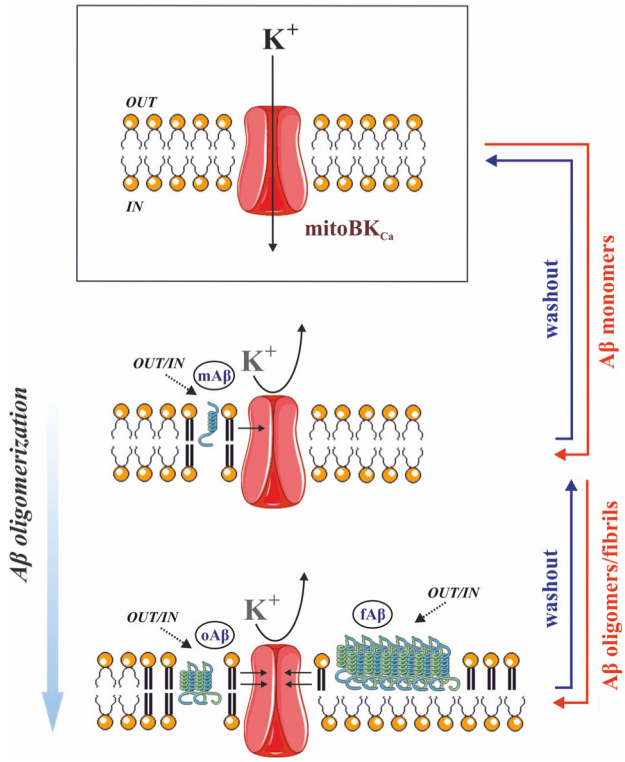

Fig. 6. A model of the membrane-mediated mitoBK$_{Ca}$ channel inhibition by Aβ. Activated mitoBK$_{Ca}$ channels transport potassium ions into mitochondria leading to cytoprotection. Aβ monomeric form (mAβ) moderately inhibits the activity of the mitoBK$_{Ca}$ channel from both sides of the membrane. Aβ in oligomeric (oAβ) or in the fibrillar form (fAβ) strongly inhibits mitoBK$_{Ca}$ channels from both sides of the membrane. Black solid straight arrows indicate the in-plane force exerted on the mitoBK$_{Ca}$ channel due to increased lipid packing in the presence of membrane-bound Aβ. Straight tails of the membrane phospholipids represent a local decrease of membrane fluidity. OUT – intermembrane space-side of the inner mitochondrial membrane. IN – matrix side of the inner mitochondrial membrane. Red arrows indicate the addition of Aβ. Blue arrows on the right indicate washout/reversibility of the Aβ effect. (For interpretation of the references to colour in this figure legend, the reader is referred to the web version of this article.)

Despite the strong evidence for a membrane-mediated action of Aβ peptides towards mitoBK$_{Ca}$ channels, we cannot completely exclude some interactions between the peptides and the channel proteins. The Aβ interactome is very large, and Aβ binding to some proteins resulted in their co-aggregation, including glyceraldehyde-3-phosphate dehydrogenase [118], α-synuclein [119], prion protein (PrP) [120,121], neuroserpin [122], and LL-37 [123]. Also, it was found that Aβ induced the aggregation of bovine serum albumin, insulin, myoglobin, cytochrome *c* or lysozyme or even simple aromatic amino acids such as Tyr, Trp, or Phe through a cross-seeding mechanism [124]. The fact that a large number of proteins interact either with Aβ or other amyloidogenic proteins [125] calls for basics mechanism what is supported by studies in which co-aggregation was also found in an artificial model of beta-sheet fibril-forming proteins [126].

Irrespective of the fact that some peptide-protein interactions between Aβ and BK$_{Ca}$ channels can take place, we argue that the membrane-mediated inhibition mechanism is more plausible. First, the inhibition was caused by all aggregate forms of Aβ. Second, the blocking effect of Aβ was observed, irrespective of the side of the membrane to which it was applied. Third, the inhibition was similar for both enantiomeric forms. Moreover, Aβ-membrane interaction seems to be more physiologically relevant. Based on our results, we propose a simple membrane-mediated mechanism in which the area occupied by Aβ at the membrane determines the extent of mitoBK$_{Ca}$ channel inhibition (Fig. 6).

5. Conclusions

We have provided strong evidence that Aβ blocks the mitoBK$_{Ca}$ channel by a membrane-mediated mechanism. We also argue that the results of our studies have a broader impact on the understanding of AD etiology, as the mitoBK$_{Ca}$ channel could be considered not only a defined target in mitochondria but also as a common model of other BK$_{Ca}$ channel isoforms, such as those located in lysosomes and the plasma membrane. Furthermore, in the prevalent model of AD, oligomers of Aβ are considered to be the main neurotoxic species; however, in the context of our studies, the monomers and amyloid fibrils might also contribute to the progression of AD by exerting a modulatory effect on membrane components.

Funding

This work was supported by International Visegrad Fund Scholarship to Kravenska Y. and the National Science Centre (Poland) [grant no. 2017/26/M/NZ3/00727] to Koprowski P.

Declaration of competing interest

The authors declare that they have no known competing financial interests or personal relationships that could have appeared to influence the work reported in this paper.

Acknowledgments

This work was supported by International Visegrad Fund Scholarship to Kravenska Y. and the National Science Centre (Poland) [grant no. 2017/26/M/NZ3/00727] to Koprowski P. The authors would like to thank Piotr Bednarczyk (Department of Physics and Biophysics, Warsaw University of Life Sciences, Warsaw, Poland) and Volodymyr Yavorsky (Department of Biophysics of Ion Channels, Bogomoletz Institute of Physiology NASU, Kyiv, Ukraine) for providing helpful feedback on data processing and results representation.

Appendix A. Supplementary data

Supplementary data to this article can be found online at https://doi.org/10.1016/j.bbamem.2020.183337.

References

[1] D.J. Selkoe, Alzheimer's disease: genes, proteins, and therapy, Physiol. Rev. 81 (2001) 741–766, https://doi.org/10.1152/physrev.2001.81.2.741.
[2] D.J. Selkoe, Alzheimer's disease is a synaptic failure, Science 298 (2002) 789–791, https://doi.org/10.1126/science.1074069.
[3] R. Tarawneh, D.M. Holtzman, The clinical problem of symptomatic Alzheimer disease and mild cognitive impairment, Cold Spring Harb. Perspect. Med. 2 (2012) a006148, https://doi.org/10.1101/cshperspect.a006148.
[4] D.R. Thal, J. Walter, T.C. Saido, M. Fändrich, Neuropathology and biochemistry of Aβ and its aggregates in Alzheimer's disease, Acta Neuropathol. 129 (2015) 167–182, https://doi.org/10.1007/s00401-014-1375-y.
[5] R.N. Rambaran, L.C. Serpell, Amyloid fibrils. Abnormal protein assembly, Prion 2 (2008) 112–117, https://doi.org/10.4161/pri.2.3.7488.
[6] J.T. Jarrett, E.P. Berger, P.T. Lansbury, The C-terminus of the β protein is critical in amyloidogenesis, Ann. N. Y. Acad. Sci. 695 (1993) 144–148, https://doi.org/10.1111/j.1749-6632.1993.tb23043.x.
[7] G. Di Fede, M. Catania, E. Maderna, R. Ghidoni, L. Benussi, E. Tonoli, G. Giaccone, F. Moda, A. Paterlini, I. Campagnani, S. Sorrentino, L. Colombo, A. Kubis, E. Bistaffa, B. Ghetti, F. Tagliavini, Molecular subtypes of Alzheimer's disease, Sci. Rep. 8 (2018) 3269, https://doi.org/10.1038/s41598-018-21641-1.
[8] M.E. Clementi, S. Marini, M. Coletta, F. Orsini, B. Giardina, F. Misiti, Aβ(31–35) and Aβ(25–35) fragments of amyloid beta-protein induce cellular death through apoptotic signals: role of the redox state of methionine-35, FEBS Lett. 579 (2005) 2913–2918, https://doi.org/10.1016/J.FEBSLET.2005.04.041.
[9] C.J. Pike, A.J. Walencewicz, C.G. Glabe, C.W. Cotman, In vitro aging of beta-amyloid protein causes peptide aggregation and neurotoxicity, Brain Res. 563

(1991) 311–314, https://doi.org/10.1016/0006-8993(91)91553-d.
[10] D.H. Small, S.S. Mok, J.C. Bornstein, Alzheimer's disease and Abeta toxicity: from top to bottom, Nat. Rev. Neurosci. 2 (2001) 595–598, https://doi.org/10.1038/35086072.
[11] D.M. Walsh, D.J. Selkoe, Aβ oligomers – a decade of discovery, J. Neurochem. 101 (2007) 1172–1184, https://doi.org/10.1111/j.1471-4159.2006.04426.x.
[12] C. Haass, D.J. Selkoe, Soluble protein oligomers in neurodegeneration: lessons from the Alzheimer's amyloid β-peptide, Nat. Rev. Mol. Cell Biol. 8 (2007) 101–112, https://doi.org/10.1038/nrm2101.
[13] M.P. Lambert, A.K. Barlow, B.A. Chromy, C. Edwards, R. Freed, M. Liosatos, T.E. Morgan, I. Rozovsky, B. Trommer, K.L. Viola, P. Wals, C. Zhang, C.E. Finch, G.A. Krafft, W.L. Klein, Diffusible, nonfibrillar ligands derived from $A\beta_{1-42}$ are potent central nervous system neurotoxins, Proc. Natl. Acad. Sci. 95 (1998) 6448–6453, https://doi.org/10.1073/pnas.95.11.6448.
[14] S. Oddo, A. Caccamo, J.D. Shepherd, M.P. Murphy, T.E. Golde, R. Kayed, R. Metherate, M.P. Mattson, Y. Akbari, F.M. LaFerla, Triple-transgenic model of Alzheimer's disease with plaques and tangles: intracellular Abeta and synaptic dysfunction, Neuron 39 (2003) 409–421, https://doi.org/10.1016/s0896-6273(03)00434-3.
[15] D. Mossmann, F.-N. Vögtle, A.A. Taskin, P.F. Teixeira, J. Ring, J.M. Burkhart, N. Burger, C.M. Pinho, J. Tadic, D. Loreth, C. Graff, F. Metzger, A. Sickmann, O. Kretz, N. Wiedemann, R.P. Zahedi, F. Madeo, E. Glaser, C. Meisinger, Amyloid-β peptide induces mitochondrial dysfunction by inhibition of preprotein maturation, Cell Metab. 20 (2014) 662–669, https://doi.org/10.1016/J.CMET.2014.07.024.
[16] Y.V. Kravenska, V.V. Chopovska, O.M. Yavorska, O.O. Lukyanetz, The role of mitochondria in the development of Alzheimer's disease, Taurian Medico-Biological Her 15 (2012) 147–149 http://dspace.nbuv.gov.ua/bitstream/handle/123456789/57521/38-Kravenska.pdf?sequence=1.
[17] W. Hu, Z. Wang, H. Zheng, Mitochondrial accumulation of amyloid β (Aβ) peptides requires TOMM22 as a main Aβ receptor in yeast, J. Biol. Chem. 293 (2018) 12681–12689, https://doi.org/10.1074/jbc.RA118.002713.
[18] L. Pagani, A. Eckert, Amyloid-Beta interaction with mitochondria, Int. J. Alzheimers Dis. 2011 (2011) 925050, , https://doi.org/10.4061/2011/925050.
[19] Y.G. Kaminsky, L.A. Tikhonova, E.A. Kosenko, Critical analysis of Alzheimer's amyloid-beta toxicity to mitochondria, Front. Biosci. Landmark Ed. 20 (2015) 173–197, https://doi.org/10.2741/4304.
[20] E.V. Kravenska, V.V. Ganzha, E.N. Yavorskaya, E.A. Lukyanetz, Effect of cyclosporin A on the viability of hippocampal cells cultured under conditions of modeling of Alzheimer's disease, Neurophysiology 48 (2016) 246–251, https://doi.org/10.1007/s11062-016-9595-5.
[21] X.-J. Han, Y.-Y. Hu, Z.-J. Yang, L.-P. Jiang, S.-L. Shi, Y.-R. Li, M.-Y. Guo, H.-L. Wu, Y.-Y. Wan, Amyloid β-42 induces neuronal apoptosis by targeting mitochondria, Mol. Med. Rep. 16 (2017) 4521–4528, https://doi.org/10.3892/mmr.2017.7203.
[22] D.C. Bode, M.D. Baker, J.H. Viles, Ion channel formation by amyloid-β_{42} oligomers but not amyloid-β_{40} in cellular membranes, J. Biol. Chem. 292 (2017) 1404–1413, https://doi.org/10.1074/jbc.M116.762526.
[23] D. Siemen, C. Loupatatzis, J. Borecky, E. Gulbins, F. Lang, Ca^{2+}-activated K channel of the BK-type in the inner mitochondrial membrane of a human glioma cell line, Biochem. Biophys. Res. Commun. 257 (1999) 549–554, https://doi.org/10.1006/bbrc.1999.0496.
[24] P. Bednarczyk, J.E. Kowalczyk, M. Beresewicz, K. Dołowy, A. Szewczyk, B. Zabłocka, Identification of a voltage-gated potassium channel in gerbil hippocampal mitochondria, Biochem. Biophys. Res. Commun. 397 (2010) 614–620, https://doi.org/10.1016/j.bbrc.2010.06.011.
[25] B. Kulawiak, A.P. Kudin, A. Szewczyk, W.S. Kunz, BK channel openers inhibit ROS production of isolated rat brain mitochondria, Exp. Neurol. 212 (2008) 543–547, https://doi.org/10.1016/j.expneurol.2008.05.004.
[26] Y. Cheng, E. Gulbins, D. Siemen, Activation of the permeability transition pore by Bax via inhibition of the mitochondrial BK channel, Cell. Physiol. Biochem. 27 (2011) 191–200, https://doi.org/10.1159/000327944.
[27] L. Leanza, E. Venturini, S. Kadow, A. Carpinteiro, E. Gulbins, K.A. Becker, Targeting a mitochondrial potassium channel to fight cancer, Cell Calcium 58 (2015) 131–138, https://doi.org/10.1016/j.ceca.2014.09.006.
[28] A. Jafari, E. Noursadeghi, F. Khodagholi, R. Saghiri, R. Sauve, A. Aliaghaei, A. Eliassi, Brain mitochondrial ATP-insensitive large-conductance Ca^{2+}-activated K^+ channel properties are altered in a rat model of amyloid-β neurotoxicity, Exp. Neurol. 269 (2015) 8–16, https://doi.org/10.1016/j.expneurol.2014.12.024.
[29] D. Gavello, C. Calorio, C. Franchino, F. Cesano, V. Carabelli, E. Carbone, A. Marcantoni, Early alterations of hippocampal neuronal firing induced by Abeta42, Cereb. Cortex 28 (2016) 433–446, https://doi.org/10.1093/cercor/bhw377.
[30] J.H. Jhamandas, C. Cho, B. Jassar, K. Harris, D. MacTavish, J. Easaw, Cellular mechanisms for amyloid β-protein activation of rat cholinergic basal forebrain neurons, J. Neurophysiol. 86 (2001) 1312–1320, https://doi.org/10.1152/jn.2001.86.3.1312.
[31] J.S. Qi, J.T. Qiao, Suppression of large-conductance Ca^{2+}-activated K^+ channels by amyloid beta-protein fragment 31-35 in membrane patches excised from hippocampal neurons, Sheng Li Xue Bao 53 (2001) 198–204.
[32] Y. Zhang, Z.-G. Shi, Z.-H. Wang, J.-G. Li, J.-Y. Chen, C. Zhang, Effects of amyloid β-peptide fragment 31–35 on the BK channel-mediated K^+ current and intracellular free Ca^{2+} concentration of hippocampal CA1 neurons, Neurosci. Lett. 568 (2014) 72–76, https://doi.org/10.1016/j.neulet.2014.03.028.
[33] P. Bednarczyk, M.R. Wieckowski, M. Broszkiewicz, K. Skowronek, D. Siemen, A. Szewczyk, Putative structural and functional coupling of the mitochondrial BK_{Ca} channel to the respiratory chain, PLoS One 8 (2013), https://doi.org/10.1371/journal.pone.0068125.
[34] H. Nieznanska, M. Bandyszewska, K. Surewicz, T. Zajkowski, W.K. Surewicz, K. Nieznanski, Identification of prion protein-derived peptides of potential use in Alzheimer's disease therapy, Biochim. Biophys. Acta Mol. Basis Dis. 1864 (2018) 2143–2153, https://doi.org/10.1016/j.bbadis.2018.03.023.
[35] A. Walewska, B. Kulawiak, A. Szewczyk, P. Koprowski, Mechanosensitivity of mitochondrial large-conductance calcium-activated potassium channels, Biochim. Biophys. Acta Bioenerg. 1859 (2018) 797–805, https://doi.org/10.1016/j.bbabio.2018.05.006.
[36] S. Bag, S. Chaudhury, D. Pramanik, S. DasGupta, S. Dasgupta, Hydrophobic tail length plays a pivotal role in amyloid beta (25-35) fibril-surfactant interactions, Proteins Struct. Funct. Bioinforma. 84 (2016) 1213–1223, https://doi.org/10.1002/prot.25069.
[37] N. Kandel, T. Zheng, Q. Huo, S.A. Tatulian, Membrane binding and pore formation by a cytotoxic fragment of amyloid β peptide, J. Phys. Chem. B 121 (2017) 10293–10305, https://doi.org/10.1021/acs.jpcb.7b07002.
[38] D.H. Cribbs, C.J. Pike, S.L. Weinstein, P. Velazquez, C.W. Cotman, All-D-enantiomers of beta-amyloid exhibit similar biological properties to all-L-beta-amyloids, J. Biol. Chem. 272 (1997) 7431–7436, https://doi.org/10.1074/jbc.272.11.7431.
[39] E. Teo, S. Ravi, D. Barardo, H.-S. Kim, S. Fong, A. Cazenave-Gassiot, T.Y. Tan, J. Ching, J.-P. Kovalik, M.R. Wenk, R. Gunawan, P.K. Moore, B. Halliwell, N. Tolwinski, J. Gruber, Metabolic stress is a primary pathogenic event in transgenic *Caenorhabditis elegans* expressing pan-neuronal human amyloid beta, Elife 8 (2019), https://doi.org/10.7554/eLife.50069.
[40] D.M.A. Oliver, P.H. Reddy, Molecular basis of Alzheimer's disease: focus on mitochondria, J. Alzheimers Dis. (2019) 1–22, https://doi.org/10.3233/JAD-190048.
[41] P.V. Martino Adami, Z. Nichtová, D.B. Weaver, A. Bartok, T. Wisniewski, D.R. Jones, S. Do Carmo, E.M. Castaño, A.C. Cuello, G. Hajnóczky, L. Morelli, Perturbed mitochondria-ER contacts in live neurons modelling Alzheimer's disease amyloid pathology, J. Cell Sci. (2019), https://doi.org/10.1242/jcs.229906 jcs.229906.
[42] A. Norambuena, H. Wallrabe, R. Cao, D.B. Wang, A. Silva, Z. Svindrych, A. Periasamy, S. Hu, R.E. Tanzi, D.Y. Kim, G.S. Bloom, A novel lysosome-to-mitochondria signaling pathway disrupted by amyloid-β oligomers, EMBO J. 37 (2018) e100241, https://doi.org/10.15252/embj.2018100241.
[43] M.F. Ribeiro, T. Genebra, A.C. Rego, C.M.P. Rodrigues, S. Solá, Amyloid β peptide compromises neural stem cell fate by irreversibly disturbing mitochondrial oxidative state and blocking mitochondrial biogenesis and dynamics, Mol. Neurobiol. 56 (2019) 3922–3936, https://doi.org/10.1007/s12035-018-1342-z.
[44] R.-Q. Liu, Q.-H. Zhou, S.-R. Ji, Q. Zhou, D. Feng, Y. Wu, S.-F. Sui, Membrane localization of β-amyloid 1–42 in lysosomes, J. Biol. Chem. 285 (2010) 19986–19996, https://doi.org/10.1074/jbc.M109.036798.
[45] L. Zheng, J. Calvo-Garrido, M. Hallbeck, K. Hultenby, J. Marcusson, A. Cedazo-Minguez, A. Terman, Intracellular localization of amyloid-β peptide in SH-SY5Y neuroblastoma cells, J. Alzheimers Dis. 37 (2013) 713–733, https://doi.org/10.3233/JAD-122455.
[46] S.F. Yan, F. Akhter, A.A. Sosunov, S.S. Yan, Identification and characterization of amyloid-β accumulation in synaptic mitochondria, Methods Mol. Biol. (2018) 415–433, https://doi.org/10.1007/978-1-4939-7816-8_25.
[47] N. Dragicevic, M. Mamcarz, Y. Zhu, R. Buzzeo, J. Tan, G.W. Arendash, P.C. Bradshaw, Mitochondrial amyloid-β levels are associated with the extent of mitochondrial dysfunction in different brain regions and the degree of cognitive impairment in Alzheimer's transgenic mice, J. Alzheimers Dis. 20 (2010) S535–S550, https://doi.org/10.3233/JAD-2010-100342.
[48] J. Lu, Y. Li, C. Mollinari, E. Garaci, D. Merlo, G. Pei, Amyloid-β oligomers-induced mitochondrial DNA repair impairment contributes to altered human neural stem cell differentiation, Curr. Alzheimer Res. 16 (2019) 934–949, https://doi.org/10.2174/1567205016666191023104036.
[49] Y. Oku, K. Murakami, K. Irie, J. Hoseki, Y. Sakai, Synthesized Aβ42 caused intracellular oxidative damage, leading to cell death, via lysosome rupture, Cell Struct. Funct. 42 (2017) 71–79, https://doi.org/10.1247/csf.17006.
[50] D. Ling, M. Magallanes, P.M. Salvaterra, Accumulation of amyloid-like $A\beta_{1-42}$ in AEL (autophagy–endosomal–lysosomal) vesicles: potential implications for plaque biogenesis, ASN Neuro 6 (2014) AN20130044, https://doi.org/10.1042/AN20130044.
[51] C. Contet, Big on BK: Current Insights into the Function of Large Conductance Voltage- and Ca^{2+}- Activated K^+ Channels at the Molecular, Cellular and Systemic Levels, Academic Press, 2016.
[52] Q. Cao, X.Z. Zhong, Y. Zou, Z. Zhang, L. Toro, X.-P. Dong, BK channels alleviate lysosomal storage diseases by providing positive feedback regulation of lysosomal Ca^{2+} release, Dev. Cell 33 (2015) 427–441, https://doi.org/10.1016/j.devcel.2015.04.010.
[53] S. Frankenreiter, P. Bednarczyk, A. Kniess, N.I. Bork, J. Straubinger, P. Koprowski, A. Wrzosek, E. Mohr, A. Logan, M.P. Murphy, M. Gawaz, T. Krieg, A. Szewczyk, V.O. Nikolaev, P. Ruth, R. Lukowski, cGMP-elevating compounds and ischemic conditioning provide cardioprotection against ischemia and reperfusion injury via cardiomyocyte-specific BK channels, Circulation 136 (2017) 2337–2355, https://doi.org/10.1161/circulationaha.117.028723.
[54] S.K. Goswami, D. Ponnalagu, A.T. Hussain, K. Shah, P. Karekar, S. Gururaja Rao, A.L. Meredith, M. Khan, H. Singh, Expression and activation of BK_{Ca} channels in mice protects against ischemia-reperfusion injury of isolated hearts by modulating mitochondrial function, Front. Cardiovasc. Med. 5 (2019), https://doi.org/10.3389/fcvm.2018.00194.
[55] R.M. Douglas, J.C.K. Lai, S. Bian, L. Cummins, E. Moczydlowski, G.G. Haddad, The

calcium-sensitive large-conductance potassium channel (BK/MAXI K) is present in the inner mitochondrial membrane of rat brain, Neuroscience 139 (2006) 1249–1261, https://doi.org/10.1016/j.neuroscience.2006.01.061.
[56] M. Piwonska, E. Wilczek, A. Szewczyk, G.M. Wilczynski, Differential distribution of Ca^{2+}−activated potassium channel beta 4 subunit in rat brain: Immunolocalization in neuronal mitochondria, Neuroscience 153 (2008) 446–460, https://doi.org/10.1016/j.neuroscience.2008.01.050.
[57] X.-H. Yan, X.-Y. Guo, F.-Y. Jiao, X. Liu, Y. Liu, Activation of large-conductance Ca^{2+}-activated K^+ channels inhibits glutamate-induced oxidative stress through attenuating ER stress and mitochondrial dysfunction, Neurochem. Int. 90 (2015) 28–35, https://doi.org/10.1016/j.neuint.2015.07.004.
[58] J.-M. Liu, Z. Yi, S.-Z. Liu, J.-H. Chang, X.-B. Dang, Q.-Y. Li, Y.-L. Zhang, The mitochondrial division inhibitor mdivi-1 attenuates spinal cord ischemia–reperfusion injury both in vitro and in vivo: involvement of BK channels, Brain Res. 1619 (2015) 155–165, https://doi.org/10.1016/J.BRAINRES.2015.03.033.
[59] K. Yamamoto, Y. Ueta, L. Wang, R. Yamamoto, N. Inoue, K. Inokuchi, A. Aiba, H. Yonekura, N. Kato, Suppression of a neocortical potassium channel activity by intracellular amyloid- and its rescue with Homer1a, J. Neurosci. 31 (2011) 11100–11109, https://doi.org/10.1523/JNEUROSCI.6752-10.2011.
[60] L. Wang, H. Kang, Y. Li, Y. Shui, R. Yamamoto, T. Sugai, N. Kato, Cognitive recovery by chronic activation of the large-conductance calcium-activated potassium channel in a mouse model of Alzheimer's disease, Neuropharmacology 92 (2015) 8–15, https://doi.org/10.1016/j.neuropharm.2014.12.033.
[61] F. Wang, Y. Zhang, L. Wang, P. Sun, X. Luo, Y. Ishigaki, T. Sugai, R. Yamamoto, N. Kato, Improvement of spatial learning by facilitating large-conductance calcium-activated potassium channel with transcranial magnetic stimulation in Alzheimer's disease model mice, Neuropharmacology 97 (2015) 210–219, https://doi.org/10.1016/j.neuropharm.2015.05.027.
[62] J.F. Disterhoft, M.M. Oh, Pharmacological and molecular enhancement of learning in aging and Alzheimer's disease, J. Physiol. 99 (2006) 180–192, https://doi.org/10.1016/j.jphysparis.2005.12.079.
[63] H. Ye, S. Jalini, S. Mylvaganam, P. Carlen, Activation of large-conductance Ca^{2+}-activated K^+ channels depresses basal synaptic transmission in the hippocampal CA1 area in APP (swe/ind) TgCRND8 mice, Neurobiol. Aging 31 (2010) 591–604, https://doi.org/10.1016/j.neurobiolaging.2008.05.012.
[64] Z. Zhang, M.X. Tang, X.R. Du, H. Li, Y.J. Feng, S.X. Ke, X.D. Tang, M. Sokabe, Q.Y. Tang, The STREX-insert in a stretch-activated BK channel from chick heart is not enough for conferring GsMTx-4 inhibitory effect on mSlo1, Biophys. J. 112 (2017) 252A, https://doi.org/10.1016/j.bpj.2016.11.1378.
[65] K. Naruse, Q.Y. Tang, M. Sokabe, Stress-axis regulated exon (STREX) in the C terminus of BK_{Ca} channels is responsible for the stretch sensitivity, Biochem. Biophys. Res. Commun. 385 (2009) 634–639, https://doi.org/10.1016/j.bbrc.2009.05.105.
[66] Z. Qi, S. Chi, X. Su, K. Naruse, M. Sokabe, Activation of a mechanosensitive BK channel by membrane stress created with amphipaths, Mol. Membr. Biol. 22 (2005) 519–527, https://doi.org/10.1080/09687860500370703.
[67] H.C. Zhao, M. Sokabe, Tuning the mechanosensitivity of a BK channel by changing the linker length, Cell Res. 18 (2008) 871–878, https://doi.org/10.1038/cr.2008.88.
[68] Q.Y. Tang, Z. Qi, K. Naruse, M. Sokabe, Characterization of a functionally expressed stretch-activated BK_{Ca} channel cloned from chick ventricular myocytes, J. Membr. Biol. 196 (2003) 185–200, https://doi.org/10.1007/s00232-003-0637-8.
[69] O. Bavi, C. Cox, M. Vossoughi, R. Naghdabadi, Y. Jamali, B. Martinac, Influence of global and local membrane curvature on mechanosensitive ion channels: a finite element approach, Membranes (Basel) 6 (2016) 14, https://doi.org/10.3390/membranes6010014.
[70] X.C. Zhang, Z. Liu, J. Li, From membrane tension to channel gating: a principal energy transfer mechanism for mechanosensitive channels, Protein Sci. 25 (2016) 1954–1964, https://doi.org/10.1002/pro.3017.
[71] T. Rasmussen, How do mechanosensitive channels sense membrane tension? Biochem. Soc. Trans. 44 (2016) 1019–1025, https://doi.org/10.1042/BST20160018.
[72] C. Yuan, R.J. O'Connell, R.F. Jacob, R.P. Mason, S.N. Treistman, Regulation of the gating of BK_{Ca} channel by lipid bilayer thickness, J. Biol. Chem. 282 (2007) 7276–7286, https://doi.org/10.1074/jbc.M607593200.
[73] H. Träuble, H. Eibl, Electrostatic effects on lipid phase transitions: membrane structure and ionic environment, Proc. Natl. Acad. Sci. U. S. A. 71 (1974) 214–219, https://doi.org/10.1073/pnas.71.1.214.
[74] Y.A. Ermakov, K. Kamaraju, K. Sengupta, S. Sukharev, Gadolinium ions block mechanosensitive channels by altering the packing and lateral pressure of anionic lipids, Biophys. J. 98 (2010) 1018–1027, https://doi.org/10.1016/j.bpj.2009.11.044.
[75] F. Sachs, Stretch-activated ion channels: what are they? Physiology 25 (2010) 50–56, https://doi.org/10.1152/physiol.00042.2009.
[76] V. Bolotina, V. Omelyanenko, B. Heyes, U. Ryan, P. Bregestovski, Variations of membrane cholesterol alter the kinetics of Ca^{2+}-dependent K^+ channels and membrane fluidity in vascular smooth muscle cells, Pflugers Arch. 415 (1989) 262–268, https://doi.org/10.1007/bf00370875.
[77] H.J. Li, Y.J. Zhang, L. Zhou, F. Han, M.Y. Wang, M.Q. Xue, Z. Qi, Chlorpromazine confers neuroprotection against brain ischemia by activating BK_{Ca} channel, Eur. J. Pharmacol. 735 (2014) 38–43, https://doi.org/10.1016/j.ejphar.2014.04.017.
[78] B. Augustynek, P. Koprowski, D. Rotko, W.S. Kunz, A. Szewczyk, B. Kulawiak, Mitochondrial BK channel openers CGS7181 and CGS7184 exhibit cytotoxic properties, Int. J. Mol. Sci. 19 (2018), https://doi.org/10.3390/ijms19020353.
[79] V. Vásquez, M. Sotomayor, J. Cordero-Morales, K. Schulten, E. Perozo, A structural mechanism for MscS gating in lipid bilayers, Science 321 (2008) 1210–1214, https://doi.org/10.1126/science.1159674.
[80] N. Mukherjee, M.D. Jose, J.P. Birkner, M. Walko, H.I. Ingólfsson, A. Dimitrova, C. Arnarez, S.J. Marrink, A. Koçer, The activation mode of the mechanosensitive ion channel, Msc L, by lysophosphatidylcholine differs from tension-induced gating, FASEB J. 28 (2014) 4292–4302, https://doi.org/10.1096/fj.14-251579.
[81] R.E. Kraichely, P.R. Strege, M.G. Sarr, M.L. Kendrick, G. Farrugia, Lysophosphatidyl choline modulates mechanosensitive L-type Ca^{2+} current in circular smooth muscle cells from human jejunum, Am. J. Physiol. Liver Physiol. 296 (2009) G833–G839, https://doi.org/10.1152/ajpgi.90610.2008.
[82] D.K. Rai, V.K. Sharma, D. Anunciado, H. O'Neill, E. Mamontov, V. Urban, W.T. Heller, S. Qian, Neutron scattering studies of the interplay of amyloid β peptide(1–40) and an anionic lipid 1,2-dimyristoyl-sn-glycero-3-phosphoglycerol, Sci. Rep. 6 (2016) 30983, https://doi.org/10.1038/srep30983.
[83] C. Lockhart, D.K. Klimov, Calcium enhances binding of Aβ monomer to DMPC lipid bilayer, Biophys. J. 108 (2015) 1807–1818, https://doi.org/10.1016/j.bpj.2015.03.001.
[84] K.J. Korshavn, A. Bhunia, M.H. Lim, A. Ramamoorthy, Amyloid-β adopts a conserved, partially folded structure upon binding to zwitterionic lipid bilayers prior to amyloid formation, Chem. Commun. (Camb.). 52 (2016) 882–885, https://doi.org/10.1039/c5cc08634e.
[85] Q. Wang, J. Zhao, X. Yu, C. Zhao, L. Li, J. Zheng, Alzheimer $A\beta_{1-42}$ monomer adsorbed on the self-assembled monolayers, Langmuir 26 (2010) 12722–12732, https://doi.org/10.1021/la1017906.
[86] D.C. Bode, M. Freeley, J. Nield, M. Palma, J.H. Viles, Amyloid-β oligomers have a profound detergent-like effect on lipid membrane bilayers, imaged by atomic force and electron microscopy, J. Biol. Chem. (2019), https://doi.org/10.1074/jbc.AC118.007195 jbc.AC118.007195.
[87] D.J. Lindberg, E. Wesén, J. Björkeroth, S. Rocha, E.K. Esbjörner, Lipid membranes catalyse the fibril formation of the amyloid-β (1–42) peptide through lipid-fibril interactions that reinforce secondary pathways, Biochim. Biophys. Acta Biomembr. 1859 (2017) 1921–1929, https://doi.org/10.1016/J.BBAMEM.2017.05.012.
[88] M. Thomaier, L. Gremer, C. Dammers, J. Fabig, P. Neudecker, D. Willbold, High-affinity binding of monomeric but not oligomeric amyloid-β to ganglioside GM1 containing nanodiscs, Biochemistry 55 (2016) 6662–6672, https://doi.org/10.1021/acs.biochem.6b00829.
[89] S.A. Kotler, P. Walsh, J.R. Brender, A. Ramamoorthy, Differences between amyloid-β aggregation in solution and on the membrane: insights into elucidation of the mechanistic details of Alzheimer's disease, Chem. Soc. Rev. 43 (2014) 6692–6700, https://doi.org/10.1039/c3cs60431d.
[90] E. Posse de Chaves, S. Sipione, Sphingolipids and gangliosides of the nervous system in membrane function and dysfunction, FEBS Lett. 584 (2010) 1748–1759, https://doi.org/10.1016/j.febslet.2009.12.010.
[91] B.R. Sahoo, T. Genjo, M. Bekier, Alzheimer's amyloid-beta intermediates generated using polymer-nanodiscs, Chem. Commun. (Camb). 54 (2018) 12883–12886, https://doi.org/10.1039/c8cc07921h.
[92] M.F. Sciacca, S.A. Kotler, J.R. Brender, J. Chen, D.K. Lee, A. Ramamoorthy, Two-step mechanism of membrane disruption by Aβ through membrane fragmentation and pore formation, Biophys. J. 103 (2012) 702–710, https://doi.org/10.1016/j.bpj.2012.06.045.
[93] K.J. Korshavn, C. Satriano, Y. Lin, Reduced lipid bilayer thickness regulates the aggregation and cytotoxicity of amyloid-β, J. Biol. Chem. 292 (2017) 4638–4650, https://doi.org/10.1074/jbc.M116.764092.
[94] C. Lockhart, D.K. Klimov, Binding of Aβ peptide creates lipid density depression in DMPC bilayer, Biochim. Biophys. Acta 1838 (2014) 2678–2688, https://doi.org/10.1016/j.bbamem.2014.07.010.
[95] M. Kubánková, I. López-Duarte, D. Kiryushko, M.K. Kuimova, Molecular rotors report on changes in live-cell plasma membrane microviscosity upon interaction with beta-amyloid aggregates, Soft Matter 14 (2018) 9466–9474, https://doi.org/10.1039/c8sm01633j.
[96] V.S. Markin, F. Sachs, Free volume in membranes: viscosity or tension? Open J. Biophys. 5 (2015) 80–83, https://doi.org/10.4236/ojbiphy.2015.53007.
[97] M. Morita, T. Hamada, M.C. Vestergaard, M. Takagi, Endo- and exocytic budding transformation of slow-diffusing membrane domains induced by Alzheimer's amyloid beta, Phys. Chem. Chem. Phys. 16 (2014) 8773–8777, https://doi.org/10.1039/C4CP00434E.
[98] T. Kubo, S. Nishimura, Y. Kumagae, I. Kaneko, In vivo conversion of racemized beta-amyloid ([D-Ser^{26}]Aβ1–40) to truncated and toxic fragments ([D-Ser^{26}]Aβ25–35/40) and fragment presence in the brains of Alzheimer's patients, J. Neurosci. Res. 70 (2002) 474–483, https://doi.org/10.1002/jnr.10391.
[99] T. Kubo, Y. Kumagae, C.A. Miller, I. Kaneko, Beta-amyloid racemized at the Ser^{26} residue in the brains of patients with Alzheimer disease: implications in the pathogenesis of Alzheimer disease, J. Neuropathol. Exp. Neurol. 62 (2003) 248–259, https://doi.org/10.1093/jnen/62.3.248.
[100] L. Millucci, L. Ghezzi, G. Bernardini, A. Santucci, Conformations and biological activities of amyloid beta peptide 25-35, Curr. Protein Pept. Sci. 11 (2010) 54–67, https://doi.org/10.2174/138920310790274626.
[101] T.A. Good, R.M. Murphy, Aggregation state-dependent binding of β-amyloid peptide to protein and lipid components of rat cortical homogenates, Biochem. Biophys. Res. Commun. 207 (1995) 209–215, https://doi.org/10.1006/BBRC.1995.1174.
[102] J.J. Kremer, M.M. Pallitto, D.J. Sklansky, R.M. Murphy, Correlation of β-amyloid aggregate size and hydrophobicity with decreased bilayer fluidity of model membranes, Biochemistry 39 (2000) 10309–10318, https://doi.org/10.1021/BI0001980.
[103] M. Suzuki, T. Miura, Effect of amyloid β-peptide on the fluidity of

phosphatidylcholine membranes: uses and limitations of diphenylhexatriene fluorescence anisotropy, Biochim. Biophys. Acta Biomembr. 1848 (2015) 753–759, https://doi.org/10.1016/j.bbamem.2014.12.003.
[104] A.H.C. Horn, H. Sticht, Amyloid-β42 oligomer structures from fibrils: a systematic molecular dynamics study, J. Phys. Chem. B 114 (2010) 2219–2226, https://doi.org/10.1021/jp100023q.
[105] R. Capone, H. Jang, S.A. Kotler, L. Connelly, F. Teran Arce, S. Ramachandran, B.L. Kagan, R. Nussinov, R. Lal, All-D-enantiomer of β-amyloid peptide forms ion channels in lipid bilayers, J. Chem. Theory Comput. 8 (2012) 1143–1152, https://doi.org/10.1021/ct200885r.
[106] G.D. Ciccotosto, D.J. Tew, S.C. Drew, D.G. Smith, T. Johanssen, V. Lal, T.-L. Lau, K. Perez, C.C. Curtain, J.D. Wade, F. Separovic, C.L. Masters, J.P. Smith, K.J. Barnham, R. Cappai, Stereospecific interactions are necessary for Alzheimer disease amyloid-β toxicity, Neurobiol. Aging 32 (2011) 235–248, https://doi.org/10.1016/j.neurobiolaging.2009.02.018.
[107] S. Dutta, A.R. Foley, C.J.A. Warner, X. Zhang, M. Rolandi, B. Abrams, J.A. Raskatov, Suppression of oligomer formation and formation of non-toxic fibrils upon addition of mirror-image Aβ42 to the natural L-enantiomer, Angew. Chemie Int. Ed. 56 (2017) 11506–11510, https://doi.org/10.1002/anie.201706279.
[108] X. Liang, J. Howard, Structural biology: Piezo senses tension through curvature, Curr. Biol. 28 (2018) R357–R359, https://doi.org/10.1016/j.cub.2018.02.078.
[109] A.H. Lewis, J. Grandl, Mechanical sensitivity of Piezo1 ion channels can be tuned by cellular membrane tension, Elife 4 (2015), https://doi.org/10.7554/eLife.12088.
[110] M.M. Maneshi, L. Ziegler, F. Sachs, S.Z. Hua, P.A. Gottlieb, Enantiomeric Aβ peptides inhibit the fluid shear stress response of PIEZO1, Sci. Rep. 8 (2018) 14267, , https://doi.org/10.1038/s41598-018-32572-2.
[111] T.M. Suchyna, S.E. Tape, R.E. Koeppe, O.S. Andersen, F. Sachs, P.A. Gottlieb, Bilayer-dependent inhibition of mechanosensitive channels by neuroactive peptide enantiomers, Nature 430 (2004) 235–240, https://doi.org/10.1038/nature02743.
[112] C. Alcaino, K. Knutson, P.A. Gottlieb, G. Farrugia, A. Beyder, Mechanosensitive ion channel Piezo2 is inhibited by D-GsMTx4, Channels 11 (2017) 245–253, https://doi.org/10.1080/19336950.2017.1279370.
[113] N. Tajima, L. Xiaoyan, M. Taniguchi, N. Kato, 24S-hydroxycholesterol alters activity of large-conductance Ca^{2+}-dependent K^+ (slo1 BK) channel through intercalation into plasma membrane, Biochim. Biophys. Acta Mol. Cell Biol. Lipids 1864 (2019) 1525–1535, https://doi.org/10.1016/j.bbalip.2019.05.010.
[114] X. Liu, N. Tajima, M. Taniguchi, N. Kato, The enantiomer pair of 24S- and 24R-hydroxycholesterol differentially alter activity of large-conductance Ca^{2+} −dependent K^+ (slo1 BK) channel, Chirality 32 (2020) 223–230, https://doi.org/10.1002/chir.23157.
[115] N.A. Barbera, B. Minke, I. Levitan, Comparative docking analysis of cholesterol analogs to ion channels to discriminate between stereospecific binding vs. stereospecific response, Channels (Austin) 13 (2019) 136–146, https://doi.org/10.1080/19336950.2019.1606670.
[116] P.T. Wong, J.A. Schauerte, K.C. Wisser, H. Ding, E.L. Lee, D.G. Steel, A. Gafni, Amyloid-β membrane binding and permeabilization are distinct processes influenced separately by membrane charge and fluidity, J. Mol. Biol. 386 (2009) 81–96, https://doi.org/10.1016/J.JMB.2008.11.060.
[117] G. Cenini, C. Rüb, M. Bruderek, W. Voos, Amyloid β-peptides interfere with mitochondrial preprotein import competence by a coaggregation process, Mol. Biol. Cell 27 (2016) 3257–3272, https://doi.org/10.1091/mbc.E16-05-0313.
[118] M. Itakura, H. Nakajima, T. Kubo, Y. Semi, S. Kume, S. Higashida, A. Kaneshige, M. Kuwamura, N. Harada, A. Kita, Y.-T. Azuma, R. Yamaji, T. Inui, T. Takeuchi, Glyceraldehyde-3-phosphate dehydrogenase aggregates accelerate amyloid-β amyloidogenesis in Alzheimer disease, J. Biol. Chem. 290 (2015) 26072–26087, https://doi.org/10.1074/jbc.M115.669291.
[119] I.F. Tsigelny, L. Crews, P. Desplats, G.M. Shaked, Y. Sharikov, H. Mizuno, B. Spencer, E. Rockenstein, M. Trejo, O. Platoshyn, J.X.-J. Yuan, E. Masliah, Mechanisms of hybrid oligomer formation in the pathogenesis of combined Alzheimer's and Parkinson's diseases, PLoS One 3 (2008) e 3135, https://doi.org/10.1371/journal.pone.0003135.
[120] J. Laurén, D.A. Gimbel, H.B. Nygaard, J.W. Gilbert, S.M. Strittmatter, Cellular prion protein mediates impairment of synaptic plasticity by amyloid-β oligomers, Nature 457 (2009) 1128–1132, https://doi.org/10.1038/nature07761.
[121] K. Nieznanski, K. Surewicz, S. Chen, H. Nieznanska, W.K. Surewicz, Interaction between prion protein and Aβ amyloid fibrils revisited, ACS Chem. Neurosci. 5 (2014) 340–345, https://doi.org/10.1021/cn500019c.
[122] K.J. Kinghorn, D.C. Crowther, L.K. Sharp, C. Nerelius, R.L. Davis, H.T. Chang, C. Green, D.C. Gubb, J. Johansson, D.A. Lomas, Neuroserpin binds Aβ and is a neuroprotective component of amyloid plaques in Alzheimer disease, J. Biol. Chem. 281 (2006) 29268–29277, https://doi.org/10.1074/jbc.M600690200.
[123] E. De Lorenzi, M. Chiari, R. Colombo, M. Cretich, L. Sola, R. Vanna, P. Gagni, F. Bisceglia, C. Morasso, J.S. Lin, M. Lee, P.L. McGeer, A.E. Barron, Evidence that the human innate immune peptide LL-37 may be a binding partner of amyloid-β and inhibitor of fibril assembly, J. Alzheimers Dis. 59 (2017) 1213–1226, https://doi.org/10.3233/JAD-170223.
[124] B.G. Anand, K.P. Prajapati, K. Kar, $A\beta_{1\text{-}40}$ mediated aggregation of proteins and metabolites unveils the relevance of amyloid cross-seeding in amyloidogenesis, Biochem. Biophys. Res. Commun. 501 (2018) 158–164, https://doi.org/10.1016/J.BBRC.2018.04.198.
[125] K.V. Biza, K.C. Nastou, P.L. Tsiolaki, C.V. Mastrokalou, S.J. Hamodrakas, V.A. Iconomidou, The amyloid interactome: exploring protein aggregation, PLoS One 12 (2017) e0173163, , https://doi.org/10.1371/journal.pone.0173163.
[126] H. Olzscha, S.M. Schermann, A.C. Woerner, S. Pinkert, M.H. Hecht, G.G. Tartaglia, M. Vendruscolo, M. Hayer-Hartl, F.U. Hartl, R.M. Vabulas, Amyloid-like aggregates sequester numerous metastable proteins with essential cellular functions, Cell 144 (2011) 67–78, https://doi.org/10.1016/j.cell.2010.11.050.